Durability studies of membrane electrode assemblies for high temperature polymer electrolyte membrane fuel cells

By

Nolubabalo Hopelorant Fanapi

A thesis submitted in fulfilment of the requirements for the degree of

Masters in Chemistry

Department of Chemistry,
University of the Western Cape

Supervisor: Dr S Pasupathi

November 2011

Declaration

I declare that "*Durability studies of membrane electrode assemblies(MEAs) for high temperature polymer electrolyte membrane fuel cells (PEMFCs)*" is my own work and that it has not been submitted for any degree or examination in any other university, and that all the sources that I have used or quoted have been indicated and acknowledged by complete references.

Nolubabalo Hopelorant Fanapi **November 2011**

Signed…….

Acknowledgements

- Appreciation goes to the Lord, my God, who has provided for me and showed me His Love, without him this would not have been a success.
- I thank my family for their emotional support and encouragement throughout the duration of this research
- I am profoundly grateful to Prof. Vladimir Linkov and the staff at the South African Institute for Advanced Material Chemistry (SAIAMC) for allowing me to conduct my research, as well as for financial support.
- I would like to express the sincere gratitude to my supervisor, Dr.Sivakumar Pasupathi for his most insightful guidance, patience, and invaluable instruction that contributed to the fulfilment of this work.
- A great thank you to Dr.Piotr Bujlo (technical assistant team) for his help.
- Thank you to Adrian Josephs (Department of Physics, UWC) for his help in SEM characterization of my samples.
- Thank you to Department of Science and Technology (DST) HySA for financial assistance.

Abstract

Polymer electrolyte membrane fuel cells (PEMFCs) among other fuel cells are considered the best candidate for commercialization of portable and transportation applications because of their high energy conversion and low pollutant emission. Recently, there has been significant interest in high temperature polymer electrolyte membrane fuel cells (HT-PEMFCs), due to certain advantages such as simplified system and better tolerance to CO poisoning. Cost, durability and the reliability are delaying the commercialization of PEM fuel cell technology. Above all durability is the most critical issue and it influences the other two issues.

The main objective of this work is to study the durability of membrane electrode assemblies (MEAs) for HT-PEMFC. In this study the investigation of commercial MEAs was done by evaluating their performance through polarization studies on a single cell, including using pure hydrogen and hydrogen containing various concentrations of CO as fuel, and to study the performance of the MEAs at various operating temperatures. The durability of the MEAs was evaluated by carrying out long term studies with a fixed load, temperature cycling and open circuit voltage degradation.

Among the parameters studied, significant loss in the performance of the MEAs was noted during temperature cycling. The effect of temperature cycling on the performance of the cell showed that the performance decreases with increasing no. of cycles. This could be due to leaching of acid from the cell or loss of electrochemically active surface area caused by Pt particle size growth. For example at 160^{o}C, a performance loss of 3.5% was obtained after the first cycle, but after the fourth cycle a huge loss of 80.8% was obtained. The in-house MEAs with Pt-based binary catalysts as anodes were studied for CO tolerance, performance and durability.

A comparison of polarization curves between commercial and in-house MEAs illustrated that commercial MEA gave better performance, obtaining 0.52 A/cm^2 at 0.5V and temperature of 160^{o}C, with in-house giving 0.39A/cm^2 using same parameters as commercial. The CO tolerance of both commercial and in-house MEA was found to be similar. In order to increase the CO tolerance of the in-house MEAs, Pt based binary catalysts were employed as anodes and the performance was investigated.

In-house MEAs with Pt/C and Pt-based binary catalysts were compared and a better performance was observed for Pt/C than Pt-alloy catalysts with Pt-Co/C showing comparable performance. At 0.5 V the performance obtained was 0.39 A/cm^2 for Pt/C, and 0.34A/cm^2,0.28A/cm^2,0.27A/cm^2 and 0.16A/cm^2 were obtained for Pt-Co/C, Pt-Fe/C, Pt-Cu/C and Pt-Ni respectively.

When the binary catalysts were tested for CO tolerance, Pt-Co showed no significant loss in performance when hydrogen containing CO was used as anode fuel. Scanning electron microscopy (SEM) revealed delamination between the electrodes and membrane of the tested and untested MEA's. Membrane thinning was noted and carbon corrosion was observed from the tested micro-porous layer between the gas diffusion layer (GDL) and catalyst layer (CL).

List of figures

List of tables

List of abbreviations

AFC	Alkaline fuel cell
AST	Accelerated stress test
CO	Carbon monoxide
DMFC	Direct methanol fuel cell
ECSA	Electrochemical surface area
EDS	Electron dispersion spectroscopy
GDL	Gas diffusion layer
IEMFC	Ion exchange membrane fuel cells
MCFC	Molten carbonate fuel cell
MEA	Membrane electrode assembly
MPL	Microporous layer
OCV	Open circuit voltage
ORR	Oxygen reduction reaction
PAFC	Phosphoric acid fuel cell
PBI	Polybenzimidazole
PEMFC	Polymer electrolyte membrane fuel cell
PTFE	Polytetrafluoroethylene
ppm	parts per million

RGF	Regenerative fuel cell
SEM	Scanning electron microscopy
SOFC	Solid oxide fuel cell
SPEFC	Solid polymer electrolyte fuel cells
TPB	Three phase boundary

List of symbols

η_{act}	Activation loss
N_{avg}	Avogadro number
q	charge
F	Faraday's constant
R_c	Internal resistance
E	Voltage

Table of contents

CHAPTER 1: Literature Review

Chapter 1: *Literature review:* Durability analysis of the membrane electrode assembly for high temperature polymer exchange membrane fuel cells.

The literature review focuses on the discussion of high temperature PEM fuel cell, its operation and general principles. Durability of PEM fuel cell is discussed, as well as degradation of membrane electrode assembly components and accelerated stressors that are applied to the fuel cell to determine the durability. This chapter is concluded by a discussion on CO investigation in PEM fuel cell.

1.1. Background to Fuel Cell Technology

Currently humankind mainly uses the heat engines such as steam turbines and internal combust engines, which combust non-regenerated fossil fuels (coal, crude oil, natural gas, etc) to generate the useful power. The energy efficiency of heat engines is low due to the limitation of Carnot cycle. The combustion of non-generated fossil fuels has resulted in severe pollution due to pollutant emissions which includes CO, SO_x, NO_x and other contaminants [1]. The combustion of non-generated fossil fuels also contributes significantly to the increase of greenhouse gas (CO_2) concentrations in the atmosphere, which intensify the prospect of global warming and threaten the existence of human beings on earth. In addition to the low efficiency and environmental concerns, the non-generated fossil fuel reserves on the planet are also limited. The limited amount of non-generated fossil fuels, increasing demand for energy and environmental concerns has driven the development of renewable energy sources as alternatives to non-generated fossil fuels and new energy conversion technologies that should be more efficient with minimal or no pollutant emissions and also compatible with the renewable energy sources for sustainable development [2]. Hydrogen

represents an alternative energy source to the non-generated fossil fuels. Fuel cells, an energy conversion technology converting chemical energy directly into electrical energy, meets the requirements for its high energy efficiency and environmental sustainability, offering other characteristics such as:

- High selectivity
- Good mechanical properties
- High power densities
- Cheap fuels which are easy to store, transport and distribute
- and Low temperature operation

When fuel cells use the hydrogen created form renewable energy sources such as solar, wind and power the only by-product is water and there are no pollutant emissions. Fuel cells can provide electrical power that can be used to a variety of applications where local electricity generation is needed. Fuel cell applications may be classified as being either mobile or stationary applications. They are powering cars, buses, boats, trains, planes, scooters and even bicycles as mobile applications [3].The interest in fuel cells will be understated if all the large car manufacturers have a FC car, either assembled in pilot scale or in the production line, and they plan to launch it before 2015 (Fig 1.1, an example of FC car).

Figure 1.1 Fuel cell car by Daimler Chrysler [4]

The primary stationary application of fuel cell technology is for the combined generation of electricity and heat, for buildings, industrial facilities or stand-by generators. There are some differences in requirements for automotive and stationary fuel cell systems, for example, size and weight requirements are very important in automobile application but not so significant in stationary applications [5].

Basics: A fuel cell consists of two electrodes separated by an electrolyte. With the help of electrocatalysts, fuel and oxidant are combined to produce electricity as shown in figure 1.2. When hydrogen is used as fuel in fuel cells on the anode side it splits into ions on the anode side (negatively charged electrode). Oxygen is the usual oxidizing reactant of the fuel cell. The reduction of the oxygen occurs on the cathode side (positively charged electrode).

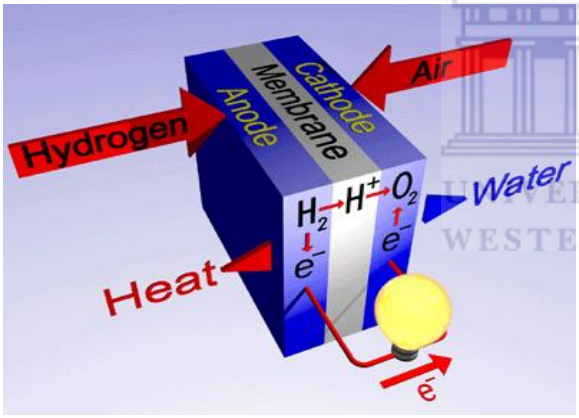

Figure 1.2 Fuel Cell diagram [6]

The reactant fuel is stored outside and fed into electrodes only when electricity is required. Continuous electricity production can be achieved by continuous feeding the fuel to the cell.

Fuel cells are generally categorized by their electrolyte that is the material sandwiched between the two electrodes. The characteristics of this material determine the optimal operating temperature and the fuel used to generate electricity. Each comes with its particular set of benefits and shortcomings. Five types of fuel cells have been under active

development, and they are phosphoric acid fuel cell (PAFC), solid oxide fuel cell (SOFC), molten carbonate fuel cell (MCFC), alkaline fuel cell (AFC) and polymer electrolyte membrane fuel cell (PEMFC). In addition to the five primary fuel classes, there are two more classes of fuel cells that are not distinguished by their electrolyte. These are direct methanol fuel cell (DMFC), distinguished by the type of fuel used, and the regenerative fuel cell (RGF) distinguished by its method of operation. The differences of the fuel cell types can be summarized as in Table 1.1.The major differences of the fuel cell types are based on the electrolyte used, the operating temperature, the charge carrier, the requirement of an external reformer, the prime cell components, and the catalyst used, water and heat management [7].

Table1.1.Main differences of fuel cell types [8]

	PEMFC	**AFC**	**PAFC**	**MCFC**	**SOFC**
Electrolyte	Ion exchange Membranes	Mobilized or immobilized potassium hydroxide	Immobilized liquid phosphoric acid	Immobilized liquid molten carbonate	Ceramic
Operating temperature	80^{o}C	65-220^{o}C	205^{o}C	650^{o}C	600-800^{o}C
Charge Carrier	H^{+}	OH^{-}	H^{+}	CO_3^{-}	O^{-}
Prime Cell components	Carbon based	Carbon based	Graphite based	Stainless based	Ceramic
Catalyst	Pt	Pt	Pt	Ni	Perovskites
Product water management	Evaporative	Evaporative	Evaporative	Gaseous Product	Gaseous Product

Among the types of fuel cells; proton exchange membrane (PEM) fuel cells technology has drawn the most attention because of its simplicity, viability, pollution free operation and quick start up [9]. It is also a serious candidate for automotive applications. High temperature

application of a proton exchange membrane fuel cell (PEMFC) can be obtained from polymers with high glass transition temperatures such as polybenzimidazole (Ma, 2004). Among various types of alternative high temperature polymer electrolyte membranes which are developed so far, phosphoric acid doped polybenzimidazole (poly [2,2-m-phenylene)-5,5-bibenzimidazole]; PBI) was reported as one of the most promising candidate.

1.2 Proton exchange membrane fuel cells

Proton exchange membrane fuel cells are also known as ion exchange membrane fuel cells (IEMFCs), solid polymer (electrolyte) fuel cells (SPEFCs) and polymer electrolyte membrane fuel cells (PEMFCs) [10].

1.2.1. Principles of Proton Exchange Membrane Fuel Cells

The proton exchange membrane also known as polymer electrolyte membrane (PEM) fuel cell uses a polymeric electrolyte. The proton conducting polymer forms the heart of the cell. The electrodes are made of porous carbon with catalytic platinum incorporated into them, are bonded to either side of the electrolyte to form a membrane electrode assembly (MEA).

The conversion of chemical energy to electrical energy in a PEM fuel cell occurs through a direct electrochemical reaction. The reaction is non-combustible. The purpose of the membrane is to conduct hydrogen ions (protons) and separate either gas to pass to the other side of the cell [11]. A schematic representation of a PEM fuel cell is shown in figure 1.3

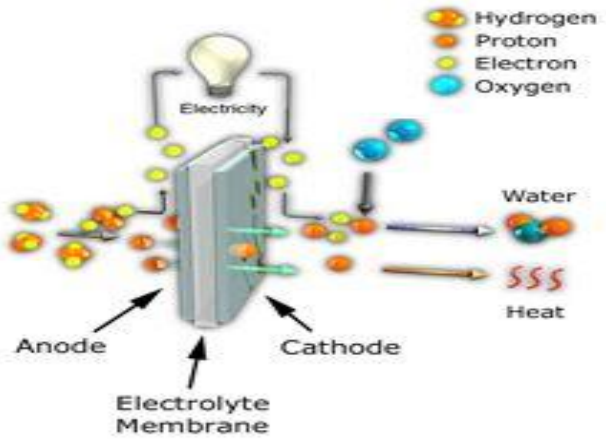

Figure 1.3 Diagram of PEM fuel cell principle [12]

Unlike in a conventional battery, the fuel and oxidant which in this case are hydrogen and air are supplied to the device from external sources. The device can thus be operated as long as the fuel and oxidant are supplied. As seen in figure 1.3 on one side of the cell the hydrogen is delivered through the flow field channel of the anode plate to the anode. On the other side of the cell, oxygen from the air is delivered through the channelled plate to the cathode. At the anode, the hydrogen molecules first come into contact with a platinum catalyst on the electrode surface. The hydrogen molecules then break apart bonding to the platinum surface forming weak H-Pt bonds. As the hydrogen molecule is broken the oxidation reaction proceed with each hydrogen atom releasing its electron which travels around the external circuit to the cathode (this flow of electrons is the one referred to as electrical current). The remaining hydrogen proton bonds with a water molecule on the membrane surface, forming a hydronium ion (H_3O^+).The hydronium ion travels through the membrane material to the cathode, leaving the platinum catalyst site free for the next hydrogen molecule [13].

At the cathode, oxygen molecules come into contact with a platinum catalyst on the electrode surface. The oxygen molecules break apart bonding to the platinum surface forming weak O-Pt bonds and allowing the reduction reaction to proceed. Each oxygen atom then leaves the platinum catalyst site combining with two electrons (which have travelled through the

external circuit) and two protons (which have travelled through the membrane) to form one molecule of water. The redox reaction has been completed. The platinum catalyst on the cathode electrode is again free for the next oxygen molecule to arrive [14]. This exothermic reaction, the formation of water from hydrogen and oxygen gases, has an enthalpy of about -286 kJ mol^{-1} of water formed. The free energy available to perform work decreases as a function of temperature, for example at 25^{o}C and 1 atmosphere, the free energy available to perform work is about -237 kJ/mole. This energy is observed as electricity and heat. The equations below show the chemical reactions taking place inside the PEM fuel cell [15].

PEM Fuel Cell:

Anode reaction: $H_2 \rightarrow 2H^+ + 2e^-$ 1.1

Cathode reaction: $^1/_2 O_2 + 2e^- + 2H^+ \rightarrow H_2O_{(l)}$ 1.2

Overall reaction: $H_2 + {}^1/_2O_2 \rightarrow H_2O_{(l)}$ 1.3

1.3. Main Components of Proton Exchange Membrane Fuel Cells

The main components of a PEMFC are as follows: (1) the ion exchange membrane; (2) the porous electrodes, which is composed of active catalyst layer (the side facing the membrane) and gas diffusion layer GDL (3) gaskets for gas tight seal and electrical insulation; (4) bipolar plates that deliver the fuel and oxidant to the reactive sites on both sides. The schematic representation of the PEMFC components is shown in Figure 1.4.

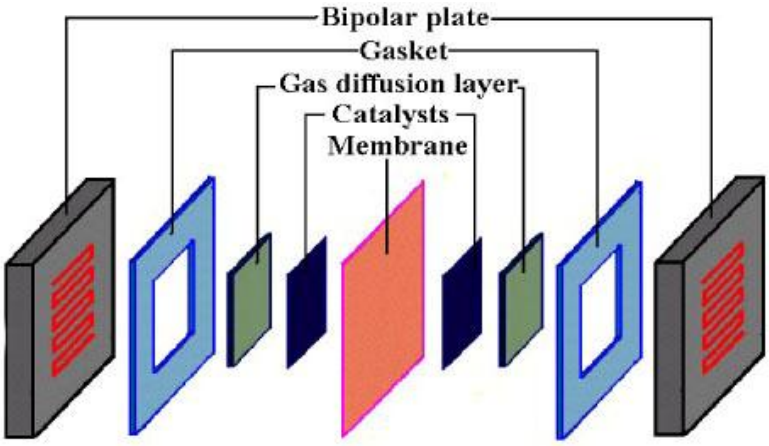

Figure 1.4 Main components of PEMFC [16]

1.3.1 Membrane Electrode Assembly (MEA)

The membrane electrode assembly (MEA) is the heart of polymer exchange membrane fuel cells (PEMFCs), and determines both fuel cell performance and durability. The MEA component materials structure and fabrication technologies play important roles in performance improvement and optimization. For example the most important component in PEMFCs is the catalyst layers because it is where the electrochemical reactions take place. MEA contains an anode gas diffusion layer (GDL) an anode catalyst layer (CL), a proton exchange membrane (PEM), a cathode catalyst layer and a cathode gas diffusion layer. An ideal MEA would allow all active catalyst sites in the catalyst layer to be accessible to the reactant (H_2 or O_2), protons and electrons and it would facilitate the effective removal of produced water from the CL and GDL.

The MEA must allow all active catalyst sites in the CL to be accessible to the reactants, protons and electrons and facilitate the effective removal of produced water from the CL and GDL. In summary the processes inside an MEA include [17]:

- Gas flow through channels

- Electron conduction
- Electrochemical reactions
- Proton transport
- Gas diffusion through porous media
- Water transport through membrane
- Water transport through porous layers
- Heat transfer

1.3.1.1 Electrolyte: Membrane

Polymer membrane electrolytes usually consist of polymer network. Membranes are proton conducting as a result of the functional groups typically acids that are attached onto this polymer network for ion exchange. In this sense the main function of the membrane in PEM fuel cells is to transport protons from the anode to the cathode. The other functions include keeping the fuel and oxidant separated, which prevents mixing of the two gases and to be able to withstand harsh conditions, including active catalysts, high temperatures or temperature fluctuations, strong oxidants and reactive radicals. Thus for these functions the ideal polymer must have excellent proton conductivity, chemical and thermal stability, strength, flexibility, low gas permeability, low water drag, fast electrode reactions and low cost [18].

1.3.1.2. Electrodes

A fuel cell electrode is the catalyst layer located between the membrane and gas diffusion layer (GDL). Electrochemical reactions take place on the catalyst surface known as the Three Phase Boundary (TPB) zone. In order for the oxygen reduction reaction (ORR) to occur the catalyst particles must be in contact with both electronic and protonic conducting materials, and there must be some passages for the transportation of the reactants to the catalytic reaction sites as well as paths for the reaction product (H_2O) to exit. In a catalyst layer,

protons travel through an electrolyte (ionomer) and electrons travel through electrically conductive solids including the catalyst itself. Therefore the catalyst particles must be in close contact with each other, the electrolyte and the adjacent GDL. The electrode requirement is that it must be porous enough to allow the gas to diffuse to the reaction sites and liquid water to go out. A diagram of catalyst layer/TPB is shown in figure 1.5 where catalyst, reactants and electrolyte meet for electrochemical reactions [19].

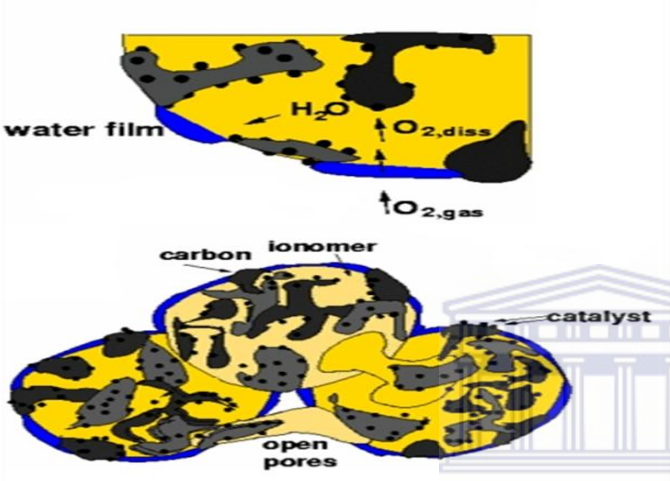

Figure 1.5 Schematic diagram showing the Three Phase Boundary (TPB) zone [20]

Platinum is considered to be the best catalyst for both the anode and cathode. The platinum catalyst is usually formed into small particles and carbon powder that has larger particles acts as a supporter for them. A widely used carbon-based powder is Vulcan X72. In this way the platinum is highly divided and spread out so that a very high proportion of the surface area will be in contact with the reactant, resulting in a great reduction of the catalyst loading with an increase in power [21].

1.3.1.3 Gas Diffusion Layers

Gas diffusion layers (GDLs) are one of the most critical components in the PEMFCs. They are directly adjacent to the bipolar plates and typically consist of two layers, the microporous substrate and a micro-porous layer (MPL). They are constructed from carbon paper or carbon cloth. Their function is to diffuse the gas to the catalyst layer. They have a porous nature that facilitates the effective diffusion of each reactant gas to the catalyst on the membrane electrode assembly. GDL also serves as an electrical connection between the carbon supported catalyst and the bipolar plate or other current collectors. GDL also helps in managing water in the fuel cell as it carries the product water away from the electrode surface.

GDL is first treated with a hydrophobic polymer such as polytetrafluoroethylene (PTFE). PTFE facilitates: (i) gases contact to the catalyst sites by preventing water from flooding within the pore volume of the backing layer, (ii) the product water to be removed from the cathode and avoids flooding and (iii) the humidification of the membrane by allowing appropriate amount of water vapour to pass through the GDL and reach the MEA and thereby improving the cell efficiency [22].

GDL also provides mechanical support to the MEA by preventing it from sagging into the flow field channels. It is also an elastic component of the MEA to handle the compression that is needed to establish the contact [23].

1.3.1.4 Gaskets

Gaskets are placed between MEAs and graphite plates to prevent gas leakage and also the direct contact between acidic electrolyte and the bipolar plate. They also prevent the electrical contact between the fuel cell stack systems. The pressure required to prevent the leak between the layers depends on the type of gasket material and that of the design. Various materials are used for fuel cell. The requirement for this material is that it must provide

excellent heat resistance, must offer superior resistance to many chemicals such as acids and also fuels. The most commonly used gasket materials are Teflon, silicone and other thermal plastics [24].

1.3.1.5 Collector plates

In a single cell the graphite plates acts as collectors conducting electrons and they act as a support structure. They are also known as bipolar plates. Their properties follow from their functions mentioned below:

- They are electrically connecting the anode and cathode of the cell thus they must be electrically conductive.
- Their primary function is to supply the reactant gases to the gas diffusion electrodes through flow channels, thus they must be impermeable to gases.
- They must be thermally conductive to conduct heat
- They must be corrosion resistant in the fuel cell environment [25].

The most common material used for bipolar plates in PEMFC is graphite. Steel and copper can also be used for bipolar plates [26].

1.4 Operation of PEM Fuel Cell

Operating conditions of PEM fuel cell include gas flow, pressure regulation, and heat and water management. High performance of a PEM fuel cell requires maintaining optimal temperature, membrane hydration and partial pressure of the reactants [27].

1.4.1 Fuel Cell Electrochemistry and Polarization Curve

The overall fuel cell reaction indicated in Eq. (1.4) is the same as the reaction of hydrogen combustion. Combustion is an exothermic process which means that there is energy that is released in the process [28]:

$$H_2 + {}^1/_2O_2 \rightarrow H_2O + \text{heat} \qquad 1.4$$

The heat of a reaction is the difference between the heat of formation of products and reactants:

$$\Delta H = h_{f,\,H2O\,(l)} - h_{f,\,H2\,(g)} - {}^1/_2 h_{f,O2(g)} = -286\ \text{kJ/mol} \qquad 1.5$$

There are some irreversible losses in energy conversion due to creation of entropy. The portion of the reaction enthalpy that can be converted to electricity corresponds to Gibbs free energy, ΔG, as shown in the equation below.

$$\Delta G = \Delta H - T\Delta S$$

The values of ΔG, ΔH and ΔS at 25°C are given in table 1.2 below.

Table 1.2 Enthalpies, entropies and Gibbs free energy for hydrogen oxidation process at 25°C [29]

	ΔH ($kJmol^{-1}$)	ΔS ($kJmol^{-1}\ K^{-1}$)	ΔG ($kJmol^{-1}$)
$H_2 + {}^1/_2O_2 \rightarrow H_2O_{(l)}$	-286.02	-0.1633	-237.34
$H_2 + {}^1/_2O_2 \rightarrow H_2O_{(g)}$	-241.98	-0.0444	-228.74

For a fuel cell the work is obtained from the transport of electrons across a potential difference and the electrical work (J/mol) is described by the following relation.

$$W = q\,E \qquad 1.6$$

Where E is the cell voltage and q is the charge (coulombs/mol). Total charge transferred in fuel cell reaction per mole of hydrogen consumed (q) is expressed as Eq. 1.7

$$q = n\, N_{avg} q_{el} = n\, F \qquad 1.7$$

Where n is the number of electrons transferred that is equal to 2 for hydrogen fuel cells, N_{avg} is the Avogadro number (6.02×10^{23}), q_{el} is the charge of an electron (1.602×10^{-19}coloumbs/electron) and F is the Faraday's constant (96485 coloumbs/mol.electron).

So the electrical work can be calculated as (Eq.1.6) [36]:

$$W = n\, F\, E \qquad 1.8$$

The work is represented by the Gibbs energy due to the electrochemical reaction:

$$W = -\Delta G \qquad 1.9$$

So the cell voltage of the system can be calculated as shown in equation 1.10 when pure hydrogen and oxygen/air gases were fed at standard conditions

$$E = -\frac{\Delta G}{nF} = \frac{2.37.34\ (\frac{kj}{mol})}{2\ (electron) x\ 96485\ (\frac{C}{mol} electron)} = 1.23\ V \qquad 1.10$$

The actual fuel cell potential (V_{cell}) is lower than the theoretical value due to various losses (ΔV_{loss}) associated with kinetics and dynamics of the processes, reactants and products. The actual potential is described as shown in equation 1.11 where E is the reversible open circuit voltage (OCV):

$$V_{cell} = E - \Delta V_{loss} \qquad 1.11$$

For the operation of a PEM fuel cell the potential is decreased from its ideal value because of several irreversible losses. These losses are:

i. Activation related losses (ΔV_{act})
ii. Ohmic losses and (ΔV_{ohm})

iii. Mass transport related losses (ΔV_{conc})

1.4.1.1 Activation loss (η_{act})

Activation loss is the dominant source of energy losses in fuel cell operation. Its effect is seen at low current densities. This loss arises due to the slowness of reactions taking place on the surface of the electrodes. There is a proportion of voltage that is lost during chemical reaction that transfers the electron to or from the electrode which mainly occurs at the cathode. It is the rate limiting reaction [30]. Due to its relationship to reaction rates, the activation polarization is also affected by the total active surface area of the catalyst surface. Losses of the active catalyst surface area during the operation due to phenomena such as particles falling off the electrode backing material or build-up of solid reaction products on the catalyst particles are the cause of this activation loss.

The loss at the cathode from the oxygen reduction reaction (ORR) is due to platinum surface area ($A_{Pt,\ el}$), platinum loading (L_{ca}), current and exchange current density (i_o) as well as the fuel cell current (i).

1.4.1.2 Ohmic loss (η_{ohmic})

Ohmic loss (η_{ohmic}) is due to the resistance to ion flow through the electrolyte membrane and the resistance to electron flow through the GDL. It is also due to an increase in contact resistances in other electrically conductive fuel cell components. Thus it can be concluded that these losses depend on the material selection. ΔV_{ohm} can be expressed by Ohm's law Equation 1.12

$$\Delta V_{ohm} = iR_c \qquad 1.12$$

Where R_c is the total internal resistance [31].

1.4.1.3 Mass transport loss or concentration loss

Mass transport losses are losses caused by mass transfer limitation rates of the reactants. Under high current densities, the kinetics of the electrode reactions is so high that the transport of reactants to the active catalyst sites limits the rate at which the fuel cell can operate [32].

The polarization curve which represents the cell voltage-current relationship is shown in (Figure 1.6) and is the standard figure of the fuel cell performance that also represents the losses.

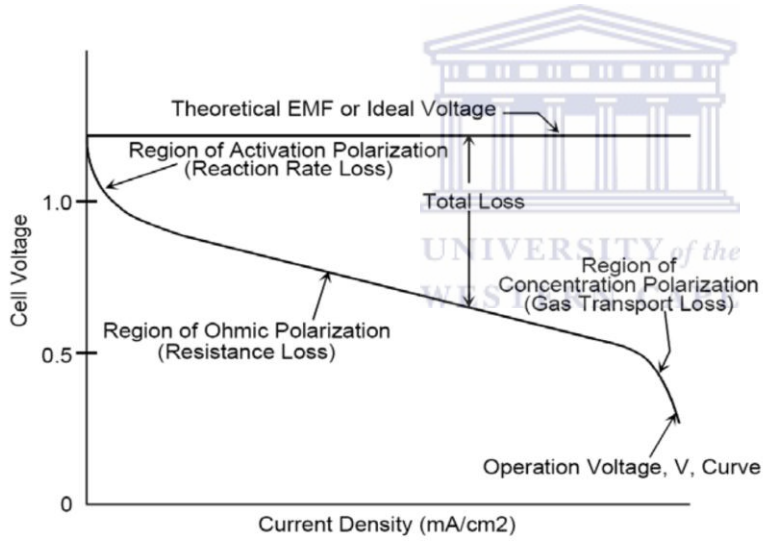

Figure 1.6 Polarization curve for fuel cell with significant losses [33]

During the fuel cell operation, the materials characteristics will inevitably change and start to degrade, As a result, the fuel cell performance observed by the polarization curve will drop. Therefore for a better fuel cell development, an understanding of how the properties change with time is important. Thus in this study membrane durability of high temperature PEM fuel cell is mainly focused.

1.4.2 Effect of Temperature on Theoretical Cell Potential

The temperature of the cell is an operating parameter that plays an important role in the cell operation. The reaction in the fuel cell is exothermal therefore it generates heat as a by-product. At high temperatures the electrochemical kinetics for both electrode reactions are enhanced. The reversible potential (E_{rev}) is very much related to temperature, for the H_2/O_2 reaction below 100^{o}C the ΔS (entropy) is negative because gases are converted to liquids thus E_{rev} decreases with increasing temperature. This effect is less pronounced above 100^{o}C when the gaseous reactants are converted to gaseous product [34].

1.5 High temperature Polymer Electrolyte Membrane

The most successful membrane is the Nafion® membrane in Figure 1.7. This membrane offers good performance below 90^{o}C under fully hydrated conditions. Also it has good chemical and mechanical stability due to the perfluorinated main chain. However the proton conductivity of this membrane is dependent on the presence of water to solvate the proton of the sulfonic groups. Consequently the operational temperature is limited to below 100^{o}C, approximately 50-90^{o}C. The gases for this membrane need to be well humidified before entering the fuel cell. During the operation of the fuel cell, water is produced at the cathode from the reduction of oxygen. Water migrates with the proton from the anode to the cathode. The excess water at the cathode diffuses back to the anode. The accumulation of excess water at the cathode side results in flooding at the cathode, preventing oxygen/air from approaching the catalyst and causing mass transfer resistance, meanwhile starvation of water in the anode side results in the decrease of conductivity. This is referred to as ‘’issue of water management’’ which significantly influences the fuel cell performance [35].

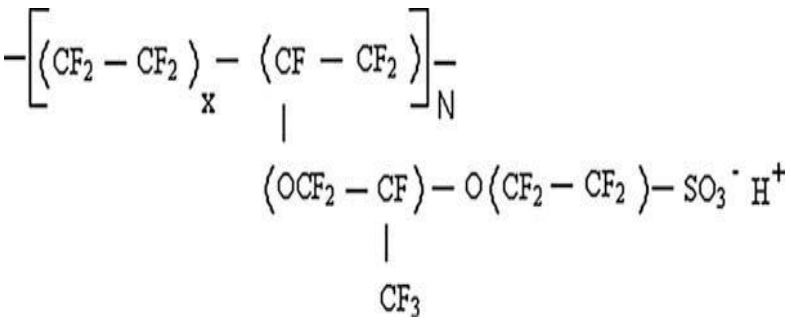

Figure 1.7 Molecular structure of Nafion® [36]

Thus the operation of PEMFC at high temperature (>120^{o}C) is desirable in several ways. The reaction kinetics is enhanced and the catalytic activity increases at higher temperatures for both electrodes. Another benefit for operating at high temperatures is the reduced poisoning effect of the catalysts by fuel impurities for example, carbon monoxide (CO). The poisoning effect has shown to be very temperature dependent that is, CO adsorption is less pronounced with increasing temperature. Nafion-based PEMFC is poisoned by CO content as low as 20-50 ppm in the fuel stream resulting in significant loss in the cell performance [37].

For a good membrane to be used for high temperature PEMFC, it is required to have the following material characteristics:

- High proton conductivity to support high currents with minimal resistive losses
- Good thermal stability
- Good mechanical strength and stability at fuel cell operating conditions
- Chemical and electrochemical stability at fuel cell operating conditions
- Good barrier for reactant species (H_2, Oxygen/Air, and small organic fuels such as methanol)
- High electrolyte transport, to maintain uniform electrolyte content
- Low cost

Among all high temperature membranes, H_3PO_4 doped-polybenzimidazole (PBI) membrane is the most widely used, showing good characteristics such as, high conductivity, good thermal stability and good fuel cell performance at temperatures up to 200^{o}C.This membrane has a high thermal stability [38]. These are some of the properties that make it a primary choice for high temperature PEMFCs.

Among many possible benzimidazole polymers is a poly (2,5benzimidazole) ABPBI with its simplest structure as shown in Figure 1.8 Poly(2.5-benzimidazole) ABPBI is the simplest benzimidazole polymer. Compared to PBI this polymer does not contain phenylene ring in the polymer backbone. This different structure gives ABPBI a higher affinity towards phosphoric acid than PBI.

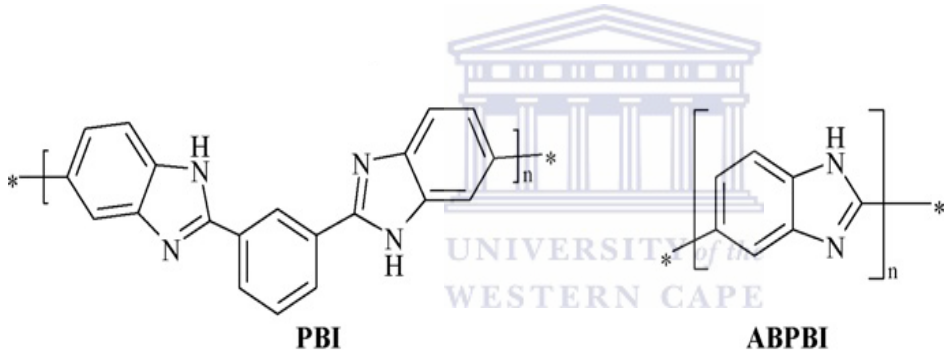

Figure 1.8 Structures of PBI and ABPBI [39]

The properties of ABPBI are summarized as follows: Like PBI it has a very high conductivity at temperatures up to 200^{o}Cunder dry conditions. This conductivity is said to increase with humidity and temperature. Since the conductivity is provided by the acid it increases also when the acid increases. It also has high thermal stability. It is said to absorb more of the phosphoric acid than the PBI.

In this study the durability of phosphoric acid doped ABPBI membranes are evaluated as the high temperature PEM for fuel cells.

There are still major remaining challenges that have to be solved before full commercialization of PEMFCs which are cost and lifetime (durability). Fuel cells must last long enough in order to serve their duties and compete with the conventional energy devices. Fuel cells are subject to high temperature, high humidity, flow of fuel and oxidant and strong acid or alkaline environment [40]. There are a number of components in the system, including the electrolytes, catalyst layers, gas diffusion layers (which comprise the membrane-electrode assemblies, MEAs), bipolar plates and current collector plates. In order to achieve good long-term performance, it is necessary for all of these components to maintain their integrity.

One of the most important factors limiting the lifetime of PEMFCs is membrane electrode assembly (MEA) degradation.

To improve durability of PEMFC without increasing cost or loosing performance the factors that determine a PEMFCs lifetime need to be studied further. The lifetime of PEMFC can be reduced by several factors including choice of materials, material composition and operating conditions. Important operational conditions that affect performance and life test include fuel cell temperature, voltage and current, humidity, pressures and impurities in the oxidant or fuel stream [41].

1.6 Polymer Electrolyte Membrane (PEM) Fuel Cell Durability

Durability is one of the most critical remaining issues impending successful commercialization of broad PEM fuel cell stationary and transportation energy applications.

Reliability of power systems based on PEM fuel cells technology is most dependent on membrane electrode assembly (MEA) durability, thus it is our main component of study. The MEA performance shows degradation over operating time, which is dependent upon materials fabrication and operating conditions [42].

1.6.1 Membrane electrode assembly degradation

In PEMFCs the electrochemical energy conversion takes place in the MEA and the MEA is therefore more prone to chemical and electrochemical degradation. Several factors can reduce the lifetime of a PEMFC, including platinum particle dissolution and sintering, carbon and chemical attachment of the membrane. These factors are highly connected to the conditions under which the fuel cell is operated. Important operating conditions include fuel cell temperature, voltage and current, pressure and humidity [43].

1.6.1.1 Carbon Support Degradation

Although carbon supported catalysts are more stable than non-supported catalyst in preventing catalyst agglomeration during cell operation, the degradation can still occur. Carbon is said to oxidize at potential near the open circuit voltage of fuel cell (1.0 V), and this oxidation rate increases with the potential. Carbon support oxidation has been shown to occur during start-up and shut down conditions in polymer electrolyte membrane fuel cells, when H_2 gas displaces air in the anode compartment after shutdown periods and momentarily increases the cathode potential to higher values. At very higher potentials the carbon support may corrode completely. The following chemical reaction describes the electrochemical oxidation of carbon.

$$C + 2H_2O \rightarrow CO_2 + 4H^+ + 4e^-$$

At temperatures of approx. (125-195^oC) platinum could catalyse the combustion of the carbon support, and that net corrosion is more severe in locations where the platinum particles reside. This leads to weakened attachment between the platinum particles and the carbon support, leading to faster platinum particle agglomeration [44].

1.6.1.2 Catalyst Corrosion

The size of the Pt-based catalyst used in PEMFC is usually in the range of 2-6 nanometers. Due to their high specific surface energy these nanoparticles tends to agglomerate into bigger particles. As these particles grow their surface energy is minimized. Pt nanoparticle agglomeration is accelerated under harsh conditions and this may result in a drop in the number of active sites.

A summary of the major failure modes in PEMFC and their likely causes are presented in Table 1.3. In most cases a combination of the inherent reactivity of component materials, harsh operating conditions, contamination and poor design/assembly is responsible for the onset of degradation.

Table 1.3 A summary of major failure modes in PEMFCs [45].

Component	**Failure modes**	**Causes**
Membrane	Chemical attack Conductivity loss Delamination from electrode	Contamination Non-uniform distribution of reactants/water/coolant Mechanical stress Drying of membrane Thermal stress
Catalyst layer	Loss of activation Decrease in mass transport rate of reactants Loss of reformate tolerance Decrease in control of water management	Sintering of electrocatalyst Corrosion of electrocatalyst Poisoning Mechanical stress Contamination Dealloying of electrocatalyst Change in hydrophobicity of materials
GDL	Decrease in mass transport rate of reactants Conductivity loss Decrease in control of water management	Degradation of backing material Mechanical stress Corrosion Change in hydrophobicity of materials
Bipolar plate	Conductivity loss Fracture/deformation	Corrosion Mechanical stress
Gasket	Mechanical failure	Corrosion Mechanical stress

1.6.1.3 Membrane degradation mechanism

Degradation of membrane in a fuel cell results from mechanical, thermal and chemical mechanisms occurring over time under harsh conditions. Mechanical damage includes membrane cracks, tears, punctures and pinholes as a result of uneven stress or other mechanical factors and this is often the main cause of early failures especially for very thin membranes. High temperatures have several advantages for PEMFCs for example, increased electrochemical kinetics and decreased susceptibility to contamination. Unfortunately the degradation of polymer membrane together with other parts of the cell increases with temperature. The chemical degradation leading to ionomer damage and loss in PEM functionality results from hydrogen peroxide that is generated through incomplete reduction in the oxygen reduction reaction (ORR). Membrane failure could also result from a combination of chemical attack, thermal attack and mechanical stresses when the fuel cell is subjected to specific extreme conditions. According to numerous experimental results, membrane degradation is strongly dependent on operating conditions such as temperature, humidity, freeze-thaw cycling, transient operation, and start-up/shut-down. All these working conditions can be employed as accelerated stressors in membrane accelerated stress tests (ASTs). Accelerated stressors for membrane degradation can be classified as follows [46]:

- Undesirable temperature
- Open circuit voltage
- Load cycling

Temperature is an important operating condition for polymer exchange membrane fuel cells. Experimental results show that material durability is one of the key challenges to overcome in order to operate PEM fuel cells at high temperatures. Beuscher et al. [72] noted that progress is needed to withstand the aggressive operating conditions of higher temperatures and/or

lower humidities, as well as longer lifetimes demanded of PEMFC applications. Relative humidity may have complex effects on component durability since both flooding and dehydration are well known factors in PEMFC performance loss. First, inadequate humidification is detrimental to the membrane, as lack of water makes the membrane brittle and fragile. At the same time higher chemical degradation of the ionomer membrane will occur under conditions continuous low humidity [47].

Open circuit voltage (OCV) without electric loading has been observed to enhance MEA degradation, especially for membrane materials with reactant gases. Peroxide radicals, which can lead to chemical decomposition of the membrane, are considered the main cause of this kind of degradation.

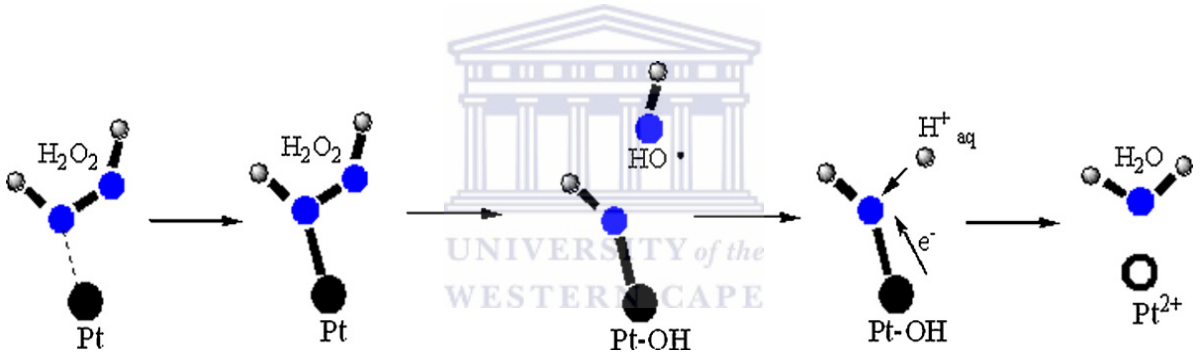

Fig.1.9. Free radical formation on the surface of Pt during the decomposition of H_2O_2[64].

Once generated, hydrogen peroxide can be readily homolysed into peroxide radicals, which are capable of breaking polymer constituent bonds. Liu and Crum [73] reported that the membrane suffered homogeneous degradation at OCV potential, resulting in massive ionomer loss and uniform thinning of the membrane throughout the active area. Inadequate water content and high temperature can also accelerate membrane thinning and pinhole formation, and lead to severe performance degradation under OCV due to more serious reactant gas crossover [48].

1.7 Carbon corrosion accelerated stress test

Carbon is an excellent material for supporting electrocatalysts, allowing mass transport of reactants and fuel cell reaction products, and providing good electrical conductivity and stability under normal conditions. Carbon corrosion weakens the attachment of Pt particles to the carbon surface and eventually lead to structural delamination and detachment of Pt particles from the carbon support which result in severe Pt agglomeration and performance degradation during long term operation [49].

1.7.1. Accelerated stressors for Carbon support degradation

The following are the accelerated stressors for carbon support:

- Fuel starvation
- Start-up/shut-down cycling
- Cold start-up at subzero temperature
- Potential control

The carbon corrosion reaction takes place at the electrode as a result of gross fuel starvation should be the direct cause of electrocatalyst's degradation. When the fuel is insufficient to provide the expected current for the PEM fuel cell, the potential value of the anode continues to increase. With fuel starvation, the cell potential will decrease to a value below normal and even drive the cell into reverse operation, with the anode potential higher than the cathode potential. Non-uniform distribution of fuel to the anode and the crossover of reactant gas through the membrane can cause carbon corrosion, in the start-up/shut-down cycling [50].

Cold start-up at subzero temperatures is another factor related to membrane PEMFC degradation induced by carbon corrosion.

The rate of carbon corrosion reaction is highly dependent on potential. During normal fuel cell operation the highest potential the cathode encounters will be the OCV, which is approximately 1.0 V. Exposure time and high potentials indirectly influence carbon oxidation because they led to the formation of platinum layers.

Carbon corrosion has been identified as a crucial degradation mechanism, especially in automotive applications. Factors such as temperature, potential cycling and humidity can affect carbon corrosion. Potential control is the most widely used technique for exploration of carbon support degradation since carbon durability is more sensitive to high potential than to other conditions [51].

1.8 Catalyst degradation mechanism

Degradation of catalyst layers (CLs) during long term operation is said to include cracking or delamination of the layer, catalyst ripening, catalyst particle migration, catalyst washout, electrolyte dissolution and carbon coarsening. All of these effects, which result either from change in the catalyst microstructure or loss of electronic or ionic contact with the active surface, can result in apparent activity loss in the catalyst layer. The electrochemical surface area of Pt is one of the most important parameters for characterizing the catalytic activity of PEM fuel cell. The widely used methods to determine electrochemical surface area (ECSA) of Pt include cyclic voltammetry (CV), CO stripping voltammetry and CO gas phase chermisorption [52].

1.8.1 Platinum agglomeration and migration

Nanoparticles have inherent tendency to agglomerate into bigger particles due to their specific surface energy. Pt nanoparticle agglomeration is accelerated under harsh operating conditions, which may result in a drop in the number of active sites and hence a decreased electrochemical surface area and this will lead to performance deterioration in PEM fuel

cells. When degraded MEAs were analyzed using transmission electron microscopy (TEM) and it was observed that changes in Pt particle structure occurred, according to the two processes : 1) small Pt particle dissolve in the ionomer phase and redeposit on larger Pt particles that are separated from each other by a few nanometers, forming a well-dispersed catalyst : 2) dissolved Pt species diffuse in the ionomer phase and subsequently precipitate in the ionomer phase of the electrode or in the membrane, this occurs through the reduction of the Pt ions by hydrogen that has crossed over from the anode and this is called the micrometer scale diffusion process[53].

Besides the increased Pt nanoparticle size, migration of Pt catalytic metals either inside the membrane or at the electrode/membrane interface also results in decreased ECSA and that leading to PEMFC performance degradation. `Rong et al. [74] found that frequent start-up/shut-down of a fuel cell led to an earlier onset of delamination between the Nafion® and the Pt/C agglomerate, which can undoubtedly limit the catalyst activity because of inferior proton transport at the interface.

Accelerated stressors for Pt catalyst degradation can be classified as follows:

- Undesirable temperature and relative humidity
- Potential control
- Load cycling
- Contamination

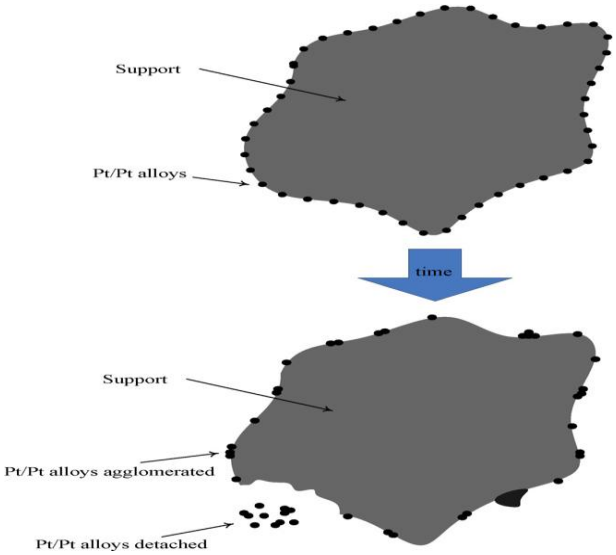

Figure 1.10 Schematic representing Pt agglomeration on carbon support and detachment from support material surface [54].

Borup et al. [75] concluded from his experimental study that the rate of Pt growth increased with increasing temperature. For high temperature PEM fuel cells using H_3PO_4 -doped poly-benzimidazole (PBI)-based MEAs, the degradation rate is also found to increase with increasing temperature. As the operating temperature is increased both the membrane and kinetic charge transfer resistances increased dramatically, mostly due to membrane and catalyst layer degradation.

It is shown from literature that the most frequently employed AST stressors for exploring MEA durability in PEM fuel cell is potential control. If the potential is lower than approximately 0.9 V, the influence is said to be caused by Pt catalyst degradation; otherwise the carbon support corrosion increases. Dam and de Bruijn's [76] experimental results showed that the Pt dissolution rate increased as the potential increased. The most serious migration of Pt occurs at the cathode side of the MEA after cycling to OCV or higher voltages. The Pt migration profile across the catalyst/membrane interface and Pt band position in the polymer membrane are thought to be dependent on potential control during

cycling, number of cycles accumulated; cell operating temperature and relative humidity. The migrated platinum particles during potential control are considered to be generated by the reduction of diffused platinum ionic species by hydrogen that has permeated through the polymer electrolyte membrane from the anode compartment [55]:

$$H_2 + Pt^{2+} \rightarrow 2H^+ + Pt$$

In PEMFC one of the most likely causes of severe degradation is contamination of the electrocatalyst or membrane. The contamination can be from the fuel or air side. For both anode and cathode catalyst layers the problem is the catalyst site poisoning and decreased catalyst activity, because even trace amounts of impurities in the reactant gas are likely to reduce fuel cell performance due to kinetic losses, especially in the long term operation. Sulphur containing species such as SO_2 are also contaminants that can create irreversible effects in the MEA and have a strong negative impact on cell performance. However for some other kind of contaminants in the feeding gas such as NO_2, the negative influence on the fuel cell is reversible when the contaminating gas is switched to pure reactant gas after poisoning. One of the major contaminants can be CO, which is contained in reformate fuel. A small amount of CO has an unacceptable negative effect on performance of a PEMFC. With only 10ppm CO in the fuel stream, a loss in performance can be observed especially at low temperature operation [56].

1.9. CO Tolerant PEM Fuel Cell

1.9.1 CO Poisoning problem in reformate fuelled PEM Fuel cell

Polymer electrolyte membrane fuel cells (PEMFCs) perform best on pure hydrogen but for many applications, especially the mobile application pure hydrogen is not yet available due to lack of practical storage techniques. Generation of hydrogen by steam reforming of various organic fuels (methanol, natural gas, gasoline and other sources) is an obvious choice. The

reformate gases contain, besides hydrogen and carbon dioxide, carbon monoxide (CO) up to 3% or even more. The CO content in the reformate gas needs to be minimised using further purification techniques such as water gas shift reactions to provide hydrogen containing 10-20 ppm CO. These traces of CO have an unacceptable negative effect on performance of the cell. Thus in this study CO tolerance in high temperature PEMFC is investigated when hydrogen containing various levels of CO is used as anode gas feed. CO needs to be cleaned from the fuel processor during generation of hydrogen by steam reforming, because it is a severe poison for the anode catalyst of the fuel cell. At high temperatures, it is reported that the CO poisoning effect is reduced because it is very temperature dependent and is less pronounced with increasing temperature [57].

1.9.2 Electrochemistry of Carbon monoxide and Hydrogen

PEMFC performance degrades when carbon monoxide (CO) is present in the fuel gas and this is referred to as CO poisoning.

Adsorption of CO on Pt is known to be associated with negative entropy, indicating that adsorption is strongly favoured at low temperature and disfavoured at high temperatures. Oxidation of hydrogen on anodic platinum catalyst is known to take place in two different steps that is dissociative chemisorption and electrochemical oxidation. The dissociative chemisorption of hydrogen molecule requires two free adjacent sites of platinum surface atoms. On the other hand, the electrochemical oxidations of the chemically adsorbed hydrogen atoms produce two free platinum sites, two hydrogen ions and two electrons. Hence the increased tolerance to CO is related to the thermodynamics of adsorption of CO and H_2 on Pt [58].

The operation of low temperature proton electrolyte membrane fuel cell requires CO concentrations as low as 5-8ppm otherwise the CO will poison the electrodes catalyst and a significant loss in fuel cell performance is observed. However hydrogen adsorption is less

exothermic than CO on Pt and H_2 adsorption on Pt requires two adsorption sites at higher temperatures increasing the temperature of fuel cells may lead to a shift towards higher H_2 coverage at the expense of CO coverage. In this study the CO tolerance is investigated by evaluating the performance of the MEAs through polarization studies, including using pure H_2 and H_2 containing various concentrations of CO at various operating temperatures [59].

1.9.3 The mechanism of hydrogen oxidation in H_2/CO on platinum

The mechanism of hydrogen oxidation in H_2/CO reformates gas on platinum is given by the following reactions in sequence [60]:

$$CO + Pt \rightarrow Pt—CO_{ads} \quad 1.13$$

$$Pt + H_2O \leftrightarrow Pt—OH_{ads} + H^+ + e^- \quad 1.14$$

$$Pt—CO_{ads} + Pt—OH_{ads} \rightarrow CO_2 + H^+ 2Pt + e^- \quad 1.15$$

$$2Pt + H_2 \rightarrow 2Pt—2H_{ads} \quad 1.16$$

$$2Pt—2H_{ads} \rightarrow 2Pt + 2H^+ + e^- \quad 1.17$$

The hydrogen oxidation reaction occurs on the free sites liberated during the time between the oxidative removal of CO illustrated in, Eq. 1.15 and CO re-adsorption from solution as shown in Eq. 1.13. It is said that at low potentials of < ~0.6V, the rate constant of CO re-adsorption is much higher than the rate constant for CO_{ads} oxidation and only a small number of platinum sites could be liberated for H_2 oxidation. The hydrogen oxidation reaction reaches a maximum at the same potential where CO_{ads} is oxidized by Pt—OH. Thus it is necessary to provide a supply of OH species to be attached on the platinum atoms covered by CO_{ads} by some other metal which does not adsorb CO. This type of catalyst is known as a bi-functional catalyst. A schematic representation of such catalyst is illustrated in Figure 1.11.

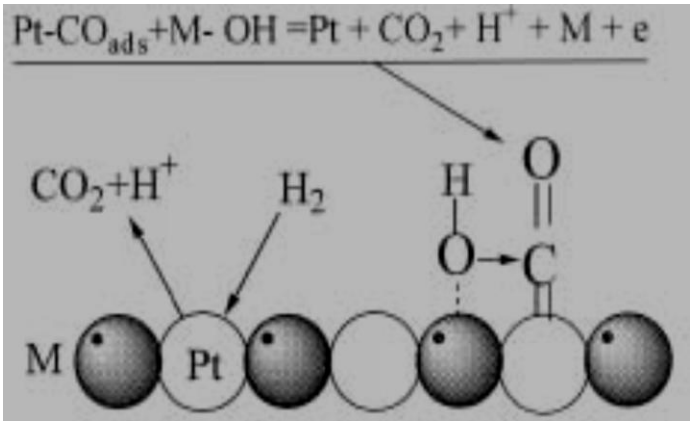

Figure 1.11 Schematic representation of bi-functional catalyst [61].

As the alloying metal (M) should provide OH for the reaction with CO_{ads}

$$Pt—CO_{ads} + OH—M \rightarrow Pt + M + CO_2 + H^+ e^- \qquad 1.18$$

it is necessary to find such metal which can provide OH at low potential. In this study Pt-based bimetallic alloy were studied as anode catalysts for CO tolerance.

1.10 Objectives

The main objective of this research is to study the durability of high temperature membrane electrode assemblies (MEAs), and the possibility to minimize the degradation by introducing binary catalysts as CO tolerant catalysts.

Investigating the hypothesis the following sub-objectives will be addressed:

- Investigating the membrane electrode assemblies by evaluating its performance through polarization studies, including using pure H_2 and H_2 containing various concentrations of CO as fuel to study the performance of the MEAs at various operating temperatures.
- Screening the durability of the MEAs by carrying out long-term studies with a fixed load, temperature cycling and OCV degradation.
- The in-house MEAs with Pt-based binary catalysts such as Pt-Co, Pt-Fe, Pt-Cu and Pt-Ni will be studied for the performance, CO tolerance and durability and compare to the commercial MEA's.
- Before and after long term performance tests the MEAs will be characterized using Scanning electron microscopy (SEM) in order to investigate the effects of long term testing on the MEA.

1.11 EXPERIMENTAL TASKS

Based on the literature review and evaluation of the performance of the membrane electrode assembly for durability studies, the following experimental tasks were approached in the study:

- Evaluation of commercial and in-house membrane electrode assemblies was done using polarization studies.

- Accelerated testing methods were applied on the MEA's.
- Characterization of the MEA using scanning electron microscopy (SEM) for identification of delamination.

1.12 INVESTIGATION OUTLINE

Chapter 2: *Methodology*

This chapter starts by discussing the polarization curves technique which is the technique used to evaluate the performance of fuel cell including the change of membrane resistance in the degradation study. Evaluation of the durability of commercial membrane electrode assembly at various operating temperatures and with CO concentrations of up to 1000ppm will be investigated. All the characterization techniques employed in the study, sample preparations and experimental parameters used are discussed in detail in this chapter.

Chapter 3: *Results and discussion*: The discussion on the results obtained through the polarization technique and microstructural characterization techniques are presented in this section.

Chapter 4 gives an insight into the durability of commercial and in-house MEAs used in the study. Comparison of performance between the commercial and in-house MEAs is done. CO tolerant catalysts have been studied and are compared to the pure platinum catalyst.

Chapter 4: *Conclusions and recommendations:* The study is concluded with a concise discussion of the objectives achieved pertaining to the study of the durability

studies of the membrane electrode assemblies (MEAs) for high temperature PEMFC.

CHAPTER 2: METHODOLOGY

Chapter 2 is dedicated to designing the experimental approach to the characterization of membrane electrode assemblies (MEAs) by polarization curves. Post-characterization of tested MEAs will also be accomplished by scanning electron microscopy (SEM). The materials used in the characterization of MEAs are listed in the table below.

Table 2.1Materials used for characterization of MEA's.

Materials and Chemicals	***Supplier***
ABPBI membrane	Fumatech
Pt/C based in-house MEAs	HySA/SAIAMC
Pt-alloy based anode MEAs	HySA/SAIAMC

Table 2.2: Chemicals used for preparation of GDL

Teflon Emulsion solution TFE 30	Electrochem, Inc
Isopropanol	Alfa-Aesar
Platinum on 40% carbon	Alfa-Aesar
Carbon paper	Electrochem, Inc

List of equipment used:

- Cell compression unit (Pragma industries)
- In-house test stand with reformate gas supply (HySA/SAIAMC)
- 25cm^2 single cell with serpentine flow field plates
- ZS Electronic load (Hocherl&Hackl)
- Ultrasonic bath (Integral systems)

- Airgun

2.1 Catalyst layer preparation

Commercial 40 wt.%Pt catalyst supported on carbon black was used for the cathode and anode catalyst for the Pt/C based in-house MEA's. To prepare the catalyst ink, a suspension was formed with the required amount of Pt/C catalyst, Nafion, ultrapure water and isopropanol as the solvent. The mixture was then dispersed by sonicating in an ultrasonic bath for 2 hrs to form an ink before being used. The catalyst ink was then spray coated onto both sides of the membrane using airgun. Pt loading used was 0.4 mg/cm^2.

2.2 GDL preparation

A Pt/C, isopropanol and 20% PTFE were mixed to make slurry. This slurry was then dispersed in an ultrasonic bath for 2hrs and stirred further for 2hrs. The ink was then spray coated on the gas diffusion layer to obtain the required loading and the membrane was sandwiched between the electrodes to form the MEA. ABPBI membrane, supplied by Fumatech is treated with H_3PO_4 at 180^{o}C for 12hrs.

Figure 2.1 A 25cm^2 active area membrane electrode assembly

2.3 Polarization curves

The most common indicator for fuel cell performance is the polarization (or current-voltage) curve. An in-house built test station was used for the experiments. There are basically two data collection modes in obtaining the polarization curve. One is to adjust the current and record the cell voltage, while the other is to adjust the cell voltage then record the current. The latter is the one used in this study for the fuel cell performance data collection. The MEA power density (cell voltage x current density) can be plotted as a function of current density. From the power density curve, the maximum power density of the fuel cell can be known [62].

The cell performance (polarization curve) strongly depends on operating conditions such as temperature, pressure, gas flow rates and other operating conditions. Normally the performance increases with increasing temperature, pressure and gas flow rate.

A Lab View control program was used to control the test bench, including the load and the feed gas composition.

2.4 Electrochemical characterization of MEAs

2.4.1 Evaluation of MEAs in a single cell

MEAs were placed in a single cell (25cm^2 active area) with a serpentine flow field. Pure hydrogen and Air was fed to the anode and cathode, respectively at flow rates of 0.5 l/min (hydrogen) and 1.00 l/min (air). The temperature in the heating tubes was controlled by temperature controllers.

An electric load connected to a computer was used to evaluate the cells. The MEAs were activated until stable performance was observed with pure hydrogen and air flowing through the cell at 160^{o}C as operating temperature.

The MEAs were activated by first purging the cell with Nitrogen (N_2) gas up to the temperature of 160^{o}C, and then H_2 and air were fed when the temperature was reached. Constant flow rates of 0.5 slpm and 1 slpm for H_2 and air respectively were used in all the experiments.

The operation of the fuel cell in this study was performed under dry conditions; this means that the gases were not humidified. During dry conditions, the hydrogen and air was controlled by a mass flow controller, and supplied through the heating tubes to the cell.

2.5 Structural characterization of MEAs by Scanning Electron Microscopy

Scanning electron microscopy (SEM) is an imaging technique that is capable of producing a three dimensional profiles of material surfaces. SEM is used in this study to characterize the morphology of the MEA sample. The sample's surface is investigated by scanning it with a high-energy beam of electrons. The electrons emitted from an electron gun in the microscope hit the sample under investigation and produce signals that contain information about the object's surface topography and composition. The SEM is able to produce very high-resolution images of the sample's surface. The high-resolution achievable with the SEM and a large depth of field provided make the instrument become useful to examine the effect of different processing techniques on material morphology [63]; MEA layers in particular. In this work, the SEM was used to compare and investigate the microstructure of fresh and degraded MEA's. Samples were fitted into the vacuum chamber of the microscope (Hitachi X-650 SEM) using GENESIS software. SEM imaging allows observation of general surface defects, thickness of each layer, separation between the MEA layers, and presence of metal contaminants and relative concentration of elements. The MEA samples were cut into small squares and then supported on a conductive carbon tape and mounted on the sample tub. No sputter coating was required as all the samples were electron conductive. Samples were fitted

into the vacuum chamber of the microscope. Operating parameters for the SEM-EDS analysis are given as follows:

Working distance: 15mm

Accelerating gun filament: Tungsten

Accelerating voltage: 25 KeV

Filament current: 75-80 Ma

2.6 Performance and durability assessment

The most common way to characterize fuel cells is by obtaining polarization curves. The polarization curves will be used to evaluate degradation and to compare tests with different operating conditions. In order to investigate degradation without having to operate the cell for thousands of hours, the tests can be done under accelerated conditions. Polarization curves are therefore taken at different stages during the accelerated tests. The following parameters are applied in this research for the accelerated test conditions. (1) Elevated temperature, (2) Open circuit voltage (OCV) (3) start-up/shut-down cycling (4) cycling conditions such as temperature and load (current).

2.6.1 Open circuit voltage (OCV)

Open circuit voltage (OCV) without electric loading enhances MEA degradation. Peroxide radicals (from hydrogen peroxide), which can lead to chemical decomposition of the membrane, are considered the main cause of this kind of degradation. Hydrogen peroxide can be generated either through the incomplete reduction of oxygen at the cathode under normal operating conditions, or the reaction of hydrogen and oxygen when significant gas crossover occurs at the anode catalyst/membrane interface under OCV. Once the hydrogen peroxide radicals are formed they are homolysed into peroxide radicals, which are capable of breaking

polymer constituent bonds. Liu and Crum reported that the membrane suffered homogeneous degradation at OCV potential, resulting in massive ionomer loss and uniform thinning of the membrane through the active area [64].

2.6.2 Start-up/Shut-down

Fuel cell is expected to experience multiple start-up and shut-down and this can result to carbon corrosion, this carbon corrosion is caused by the non-uniform distribution of fuel to the anode. Under conditions of a prolonged shutdown, unless the cell is purged properly, the hydrogen crossover from anode to cathode will empty out the anode chamber and result in an air-field flow channel. In this case, the starting flow of fuel will induce a transient condition in which fuel exists at the inlet but the exit is still fuel-starved. As a result, starting and stopping the fuel cell can induce considerable damage to the cell [65].

2.6.3 Temperature cycling

Temperature cycling is done to determine the resistance of the cell to temperature extremes. It is performed by exposing the cell to various temperatures from high to low temperature and vice versa [66] particularly from 160^{o}C to 40^{o}C. It is observed that as the cell undergoes further cycling between various temperatures the performance decrease. Further investigation in this area is necessary to identify the reasons for the significant drop in performance with cycling.

Chapter 3: Results and Discussion

In this chapter the experimental evaluation for the durability of high temperature MEAs was studied. Pt/C based commercial and in-house MEAs were tested for performance at various temperatures and long term studies were done using pure hydrogen. Hydrogen containing CO concentration was used to investigate the CO tolerance. Pt-alloy based catalysts for anode were tested as CO tolerant catalyst on in-house MEA's. Gas flow rates of 0.5 slpm (H_2) and 1.00 slpm (Air) were applied for all the tests.

3.1 Polarization studies

3.1.1 Performance of the commercial MEA

Figure 3.1 shows the polarization curve of a commercial MEA at 160^{o}C which is the ideal operating temperature for the combined heat and power (CHP) application system. When it comes to high temperature PEMFC (HT-PEMFC) the potential is for combined heat and power (CHP) because at high temperatures the temperature of the heat produced is higher which lead to easier heat management and better utilization with smaller heat exchangers. The other advantage is that in the reforming process steam is needed thus steam can be produced by the heat of the fuel cell as the temperature is high enough [67].

From the graph it can be seen that at 0.5 V the cell obtained a current density of 0.52 A/cm^2 with the power output of 0.23 W/cm^2. At the operating temperature of 160^{o}C it is where the long term durability tests are carried out to evaluate the performance of the cell.

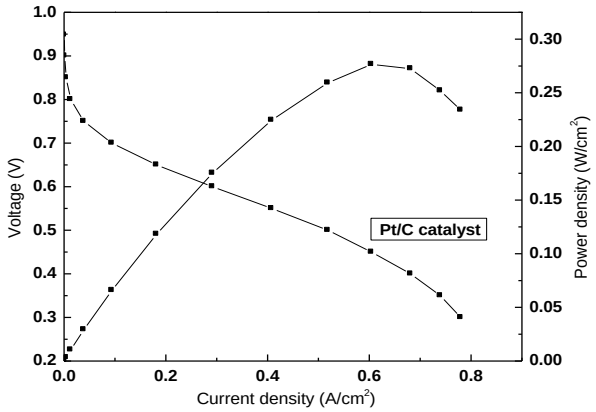

Figure 3.1 Polarization graph showing cell voltage and power density versus current density for a commercial MEA at 160^{o}C (Anode/Cathode flow rate = 0.5slpm /1.00slpm respectively).

From figure 3.1 the three losses in fuel cell are observed from the polarization curve which is activation loss, ohmic and mass transport losses. Activation loss is due to slowness of the reactions taking place on the surface of the electrodes and the effects of these losses occur at low current densities. Figure 3.1 indicates that the activation loss is one of the major contributors to the low performance of HTPEMFC MEAs, which can be related to the deactivation of the catalyst. Since the Hispec catalyst used in this study is well known for its performance in low temperature fuel cells, the deactivation in this case is mainly caused by the adsorption of phosphoric acid onto the catalytic sites.

3.1.2 MEA performance as a function of temperature

Polarization curves were obtained using phosphoric acid AB-PBI-based MEA's at different temperatures with non-humidified hydrogen and air as reactant gases and at atmospheric pressures as shown in Figure 3.2. It can be seen that the fuel cell performance increases significantly as the temperature increases.

At the voltage of 0.5 V, the current densities obtained at different temperatures are 0.308 A/cm^2 (100^{o}C), 0.382 A/cm^2 (120^{o}C), 0.477 A/cm^2 (140^{o}C) and 0.519 A/cm^2 (160^{o}C).

It can also be observed from Figure 3.2 that the gaps between polarization curves for two adjacent temperatures decrease slightly with an increase in temperature. For example at the voltage of 0.5V, the current density difference between 120^{o}C and 140^{o}C is 0.095A/cm^2, while the current density difference between 140^{o}C and 160^{o}C is 0.042A/cm^2.The performance at 40^{o}C is found to be reasonable as this is comparable to the performance in low temperature PEMFC. This may indicate that the temperature effect on PBI based fuel cell performance is more pronounced at lower temperatures than at higher temperatures.

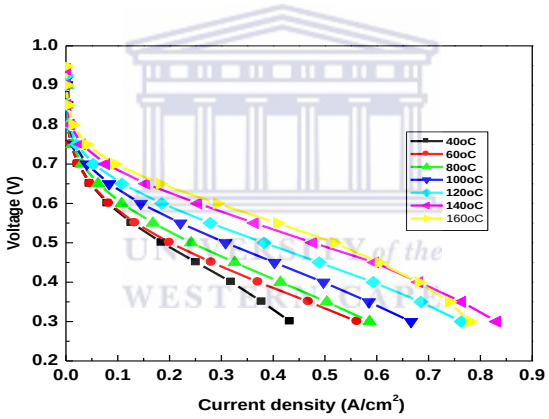

Figure 3.2 Performance of phosphoric acid ABPBI based MEA at various temperatures.

A long term performance testing of commercial MEA is shown in figure 3.3 that was operated with pure H_2/Air at constant voltage of 0.5V and 160^{o}C as operating temperature. For the durability evaluation, the cell was operated under steady-state condition at the above mentioned parameters. This method is carried out by applying a certain voltage (in this case is 0.5 V) and monitoring the drop in the performance of the cell over a period of time. A slight increase in performance was observed in the first 200min of the durability test. The

reason for the slight improvement might be due to some phosphoric acid leaving the catalyst layer leading to the catalytic sites becoming more available for electrochemical reaction. Another possibility could be the expansion of the interface for the electrochemical reaction, by opening up of the pores in the GDE. After 200 min, a stable performance was noted for the duration of the project.

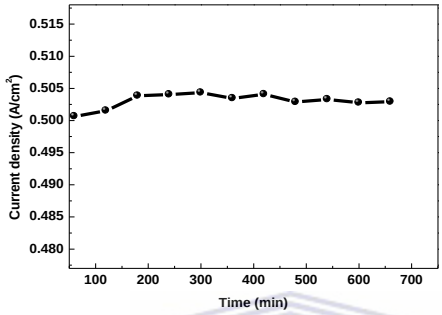

Figure 3.3 Long term performance testing of commercial MEA (V_{cell} = 0.5V, T_{cell} = 160^{o}C, Anode/Cathode flow rate = 0.5slpm /1.00slpm respectively)

3.1.3 Investigation of CO tolerance with AB-PBI based PEMFC

It is said that the presence of small amount of carbon monoxide (CO) impurities in the hydrogen-rich gas mixture produced by reforming of hydrocarbon fuels is unavoidable. CO strongly adsorbs on the carbon-supported platinum catalyst and in case of LT-PEMFCs as small as 10ppm of CO blocks the catalytically active area, thereby significantly decreasing its reactivity [68]. In order for HTPEMFC MEAs to be attractive, up to 3% CO tolerance should be achieved, which will reduce the CO cleaning step during natural gas reforming. Thus in this study various concentrations of CO were tested to investigate the maximum concentration that can be tolerated with the HTMEA when a reformate gas is used as anode feed gas. The effects of temperature for various concentrations are investigated on the current-voltage characteristics of the fuel cell.

Fuel cell performance curves with pure hydrogen and hydrogen containing carbon monoxide are shown in Figure 3.4 at an operating temperature of 160^{o}C. Concentrations of 50 ppm, 100 ppm, 200 ppm, 500 ppm and 1000 ppm were tested.

At the cell voltage of 0.5 V, the current density decreases from 0.52 A/cm^2 for pure H_2 to 0.46 A/cm^2(decreased by 11.5%) for hydrogen containing 50ppm CO, to 0.44 A/cm^2 (decreased by 15%), 0.37 A/cm^2(28.8% decrease) and 0.28 A/cm^2(46% decrease) for 100ppm, 200ppm and 1000ppm respectively. It can be seen that the current-voltage curves changes significantly as the concentration of CO is increased in the anode feed. In some of the studies reported, CO tolerance of up to 1000 ppm was shown, however it has to be noted that the operating conditions in our case is with dry H_2/Air and at atmospheric pressures which might be the reason for different tolerance levels noted in our studies.

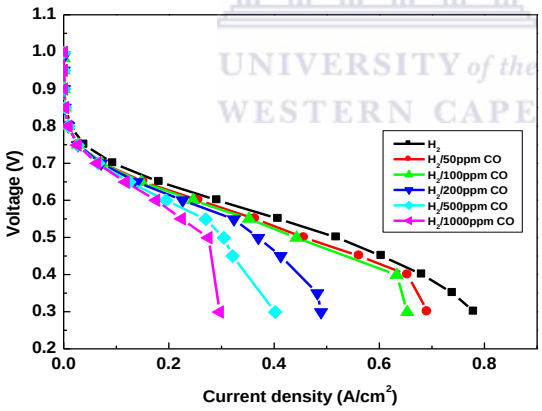

Figure 3.4 Current-Voltage performance of commercial MEA at 160^{o}C with CO concentrations indicated in the figure.

At high temperature of 180^{o}C the dissociative chemisorption mechanism of hydrogen molecules can occur further on a small fraction of the Pt catalyst surface area free of CO. Therefore more hydrogen molecules can be bonded by chemisorption on free Pt surfaces to

release more electrons and protons and therefore cell performance is improved as can be seen from figure 3.5.

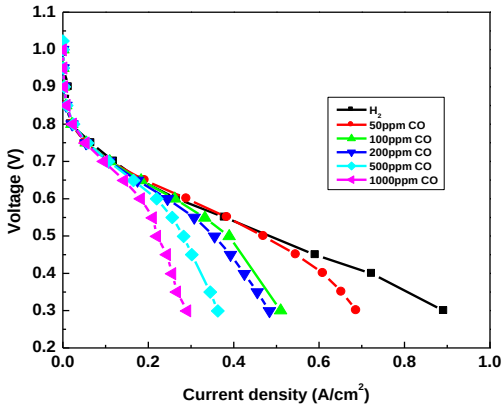

Figure 3.5 Current-Voltage performance of commercial MEA at 180°C with CO concentrations indicated in the figure.

50ppm and 100ppm CO showed only a slight deviation from the pure hydrogen polarization curve at 0.5 V, while a significant loss was observed up to below 0.3 A/cm^2 for 1000 ppm. The performance of the cell dropped from 0.49 A/cm^2 for hydrogen to 0.46 A/cm^2 for hydrogen containing 50ppm CO, to 0.44 A/cm^2 for 100 ppm. Other CO concentrations dropped to below 0.37 A/cm^2. This shows that the presence of CO concentrations above 100ppm poison the catalyst surface significantly.

3.1.4 Effect of Temperature Cycling on Performance of the Cell

The graph in figure 3.6 shows the effect of temperature cycling on the cell. Temperature cycling is carried out to understand the behaviour of the MEA during dynamic operation and to determine the resistance of the cell to temperature extremes. It is performed by exposing the cell to various temperatures from high to low temperature and vice versa. It is observed that as the cell undergoes further cycling between various temperatures the performance decreases significantly.

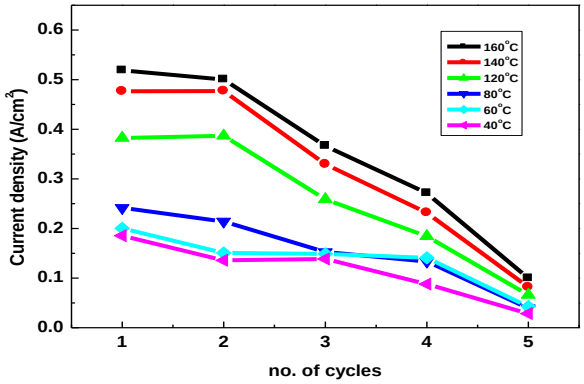

Figure 3.6 Temperature cycling graph of commercial MEA at various operating temperatures.

The graph from figure 3.6 shows that after the first cycle the current density obtained at 160°C was 0.52 A/cm^2 at the voltage of 0.5 V, then a decrease to 0.48 A/cm^2 was obtained after the second cycle. After 3 cycles at the same temperature, the cell current density decreased to 0.19 A/cm^2.

This cycling between the temperatures causes a significant loss in the overall performance of the cell. This loss in performance might be due to loss of electrochemically active surface area (ECSA) caused by the growth of Pt particle size which increased with fuel cell operating time, and leaching of the acid might have caused this decrease. Further investigation in this area is necessary to identify the reasons for the significant drop in performance with cycling. The performance loss due to temperature cycling is calculated as shown in table 3.1.

Table3.1 Table showing performance loss of the cell at 160^{o}C

No. of cycles	Performance loss (%) At 160oC	Performance loss (%) At 80^{o}C
1	3.5	11.4
2	29.4	36.9
3	47.7	44.8
4	80.8	83.6

3.1.5 The morphology of tested and untested MEAs

Delamination describes an MEA feature whereby the catalyst layer has separated from the polymer membrane electrolyte as shown in Fig. 3.7 [69]. SEM characterizations of untested and tested MEA after durability test were conducted to investigate the effects of long term testing on the MEA. The electrodes (anode and cathode) and the AB-PBI membrane were not hot pressed to make the MEA, the electrode and membrane was put together and assembled. Since the electrodes and membrane are not hot-pressed, both the fresh and tested MEA show a gap between the membrane and electrodes as shown in figure 3.7 (a) and 1(b). The thickness of the ABPBI membrane after durability test was 30.07μm, which was thinner than its original thickness of 54.4μm and this thinning is known to be due to the attack of the membrane by hydroxyl (HO•) and hydrogen peroxide (HO_2•) produced by the incomplete reduction of oxygen on the cathode side. It is known that the attack of HO• and HO_2• radicals

produced by the incomplete reduction of oxygen on the cathode side is the main factor for the oxidative degradation of the PBI membrane [70].

Untested ABPBI membrane Tested ABPBI membrane

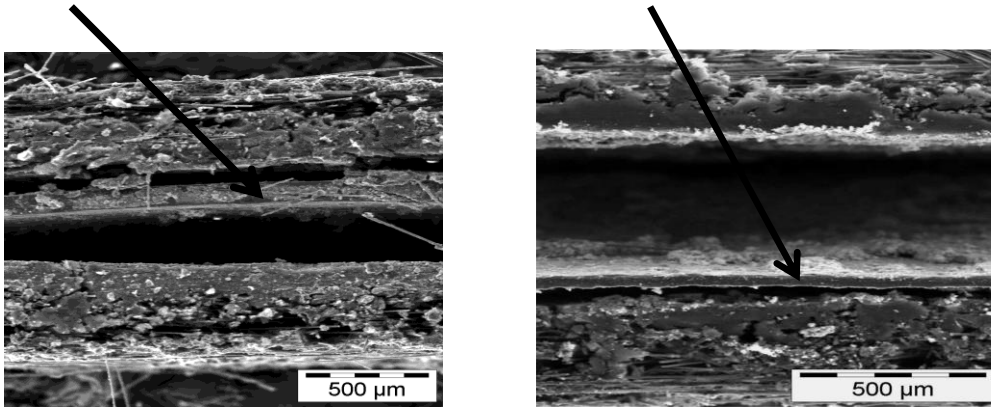

(a) Untested MEA (b) Tested MEA

Figure3.7 SEM image of MEA in cross-section (a) before durability testing: (b) after durability test

Figure 3.8 shows the GDL cross-section of untested and tested MEAs respectively. The physical changes in GDL are observed and this is due to loss of carbon as it is made of carbon based porous material including micro-porous carbon paper or carbon cloth covered by a thin micro-porous layer consisting of carbon powder. From the SEM images the untested image seems to have much of the carbon bounded on the carbon fibres. While the tested shows a loss of this carbon which might have corroded during the durability testing. Therefore the results indicate that the performance drop during long term testing is mainly due to carbon corrosion in the catalyst and GDL layers.

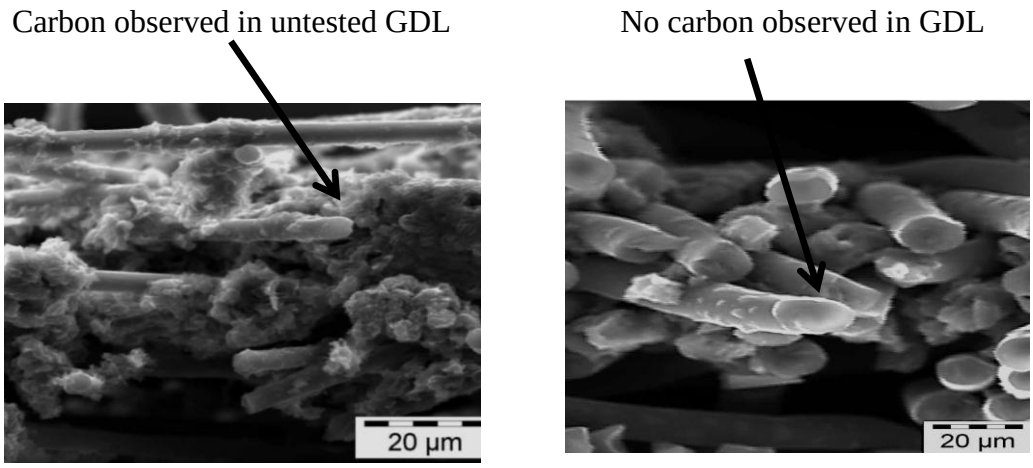

(a) Untested GDL (b) Tested GDL

Figure 3.8 SEM image of gas diffusion layer (GDL) in cross-section (a) before durability test and (b) after durability

3.1.6 Performance of in-house MEAs

The graph of cell voltage and power density versus current density in figure 3.9 shows the performance of a Pt/C catalyst based in-house MEA. When the MEA was tested at 160^{o}C a current density of 0.39 A/cm^2 was obtained at 0.5 V with a maximum power output of 0.21 W/cm^2.

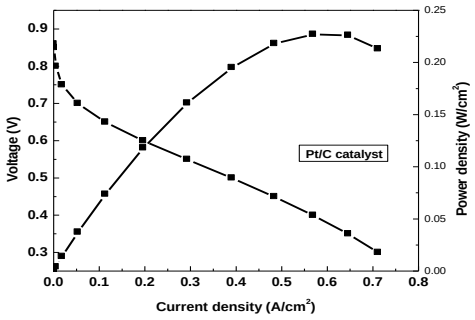

Figure 3.9 Polarization graph showing cell voltage and power density versus current density for an in-house MEA at 160^{o}C.

From figure 3.10 we can see that as the temperature increases the polarization curve shifted upward indicating that the cell performs better at higher temperature. It implies that fuel oxidation rate is higher, and as a result cell performance improvement is observed at higher temperatures. At 180^{o}C the current density obtained at 0.5 V is 0.478 A/cm^{2}, with 160^{o}C and 140^{o}C giving 0.391 A/cm^{2} and 0.304 A/cm^{2} respectively. It is observed that the cell temperature has a great impact on the performance of high temperature PEM fuel cell.

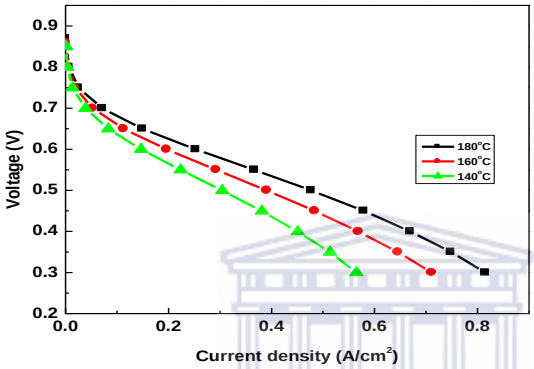

Figure 3.10 Polarization curves showing the performance of a Pt/C based in-house MEA at various temperatures.

A long term performance testing is shown in figure 3.11 for an in-house ABPBI based MEA operated with pure H_2/Air at a constant voltage (0.5 V). The performance of the MEA was monitored and slight increase in performance was observed in the first 190 min of operation, this is likely to be caused by the improved interfacial contact between electrolyte and catalyst layers. Then the performance started to decrease gradually from 0.330 to 0.325 A/cm^{2} after 550 min. This decrease in performance might be due to agglomeration of the cathode and anode catalyst during the long term test and another reason could be the leaching of a small amount of H_3PO_4 from the electrolyte. The results indicate that the phosphoric acid content in the in-house MEAs is much lesser as compared to the commercial ones.

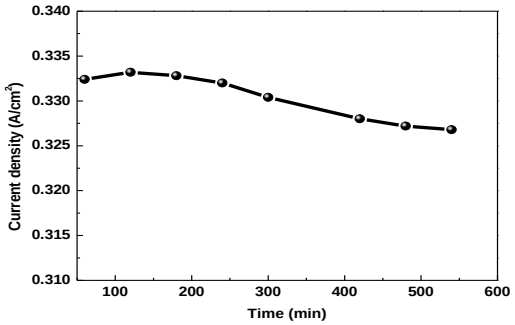

Figure 3.11 Long term performance testing of in-house MEA (V_{cell} = 0.5V, T_{cell} = 160°C, Anode/Cathode flow rate = 0.5slpm /1.00slpm respectively)

3.1.7 Investigation of CO tolerance of in-house MEAs

Figure 3.12 shows fuel cell performance curves with pure hydrogen and hydrogen containing carbon monoxide at 160°C for an in-house MEA with Pt/C as catalyst for both anode and cathode. At the cell voltage of 0.5 V the current density decreased from 0.39 A/cm^2 for hydrogen to 0.36 A/cm^2 for hydrogen containing 50ppm CO (decreased by 8%), to 0.32 A/cm^2 for 100 ppm CO (decreased by 22%), to 0.30 A/cm^2 for 200 ppm and 0.26 A/cm^2 for 1000 ppm (33%).

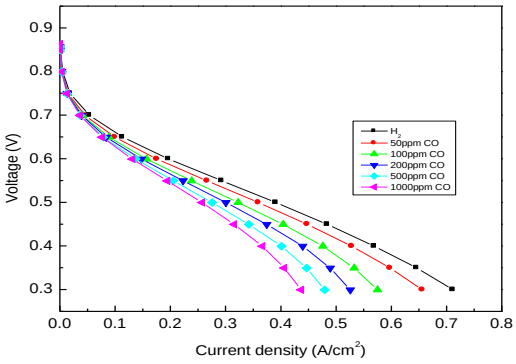

Figure 3.12 Polarization curves of a PBI-based membrane with pure hydrogen and hydrogen containing CO at 160°C. The concentrations are indicated in the figure.

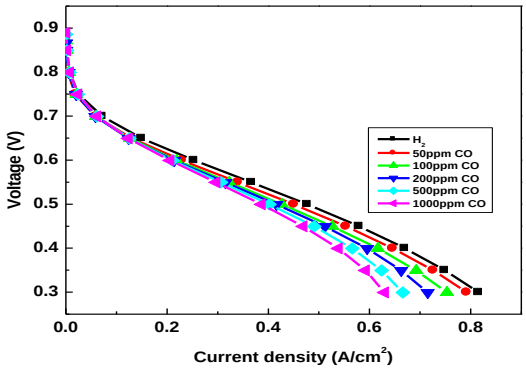

Figure 3.13 A Pt/C catalyst based in-house MEA with pure hydrogen and hydrogen containing CO at 180°C. The concentrations are indicated in the figure.

At 180°C as shown in figure 3.13, only a slight decrease in performance was observed. At the same voltage a 50 ppm CO caused a decrease in current density from 0.48 A/cm^2 to 0.45 (decreased by 6%), a drop to 0.42 A/cm^2 (13% decrease) and 0.39 A/cm^2 (19% decrease) for 200 and 1000 ppm CO was observed.

It is observed that the decrease in performance at higher temperatures with hydrogen containing CO is minimized. This is also shown by the gaps between the polarization curves when H_2 containing CO is tested at higher temperatures which show a decrease between two adjacent CO concentrations, pointing to a certain degree of tolerance at these temperatures. However, the tolerance of these MEAs has to be improved quite significantly for use with reformates without the need for CO cleaning.

3.1.8 Comparison between in-house and commercial MEAs

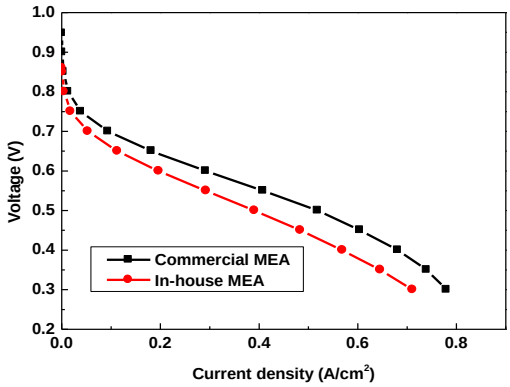

Figure 3.14 Comparison graph of Pt/C based in-house and commercial MEAs at 160°C.

The graph in figure 3.14 shows the performance between commercial and in-house MEA's at 160°C as operating temperature. The performance of in-house MEA was reasonable as compared to the commercial one where the performance of the commercial MEA was 0.52 A/cm^2 at 0.5 V, while the in-house MEA was 0.39 A/cm^2 of current density at the same voltage. Thus the difference in performance between commercial and in-house depends on the catalyst deposition during MEA preparation and the thickness of the GDL used. Spraying techniques also play a role on the performance difference between the two MEA's.

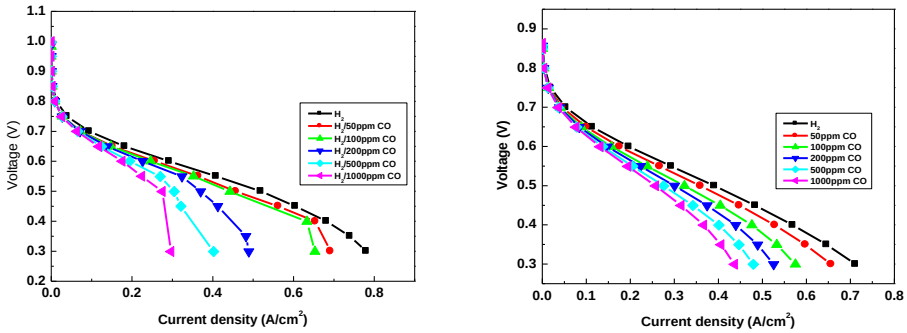

(a) (b)

Figure 3.15 Polarization curves indicating the CO tolerance at 160°C when (a) commercial and (b) in-house MEAs were tested.

In a commercial MEA as shown in Figure 3.15, 50 ppm CO in hydrogen resulted in a decrease of 12% in current density at the cell voltage of 0.5 V, 100 ppm CO of 16%, 200 ppm of 29% and 1000 ppm CO of 46% With the in-house MEA, the current density decreased from 0.39 A/cm^2 for H_2 to 0.36 A/cm^2 (decreased by 8%) for hydrogen containing 50ppm CO, to 0.32 A/cm^2 (decreased by 18%) for 100 ppm CO, to 0.30 A/cm^2 (decreased by 23%) for 200 ppm and to 0.26 A/cm^2 (decreased by 33%) for 1000 ppm. Therefore, similar drop in the performance of the MEAs was noted for both in-house and commercial MEAs with increasing CO concentration.

3.1.9 Pt-alloys based anode catalysts

In this study four binary Pt alloys (Pt-Co/C, Pt-Cu/C, Pt-Fe/C and Pt-Ni/C) supported on carbon was studied for CO tolerance and their durability.

Pt-Ru is well known to exhibit better performance for the hydrogen oxidation reaction in the presence of CO, especially for low temperature fuel cells. In our study other Pt based binary catalysts, provided above, which were reported to have better CO tolerance were evaluated

for their tolerance and durability. The study of these catalysts is to find out if a reformate gas can be used as anode gas feed without any significant loss from the cell.

I. Pt-Cu/C anode catalyst

The graph in figure 3.16 shows the performance of a Pt-Cu/C as anode catalyst for the in-house MEA. The current density obtained at 0.5 V is only 0.268 A/cm^2 with a maximum power density of 0.178 W/cm^2.

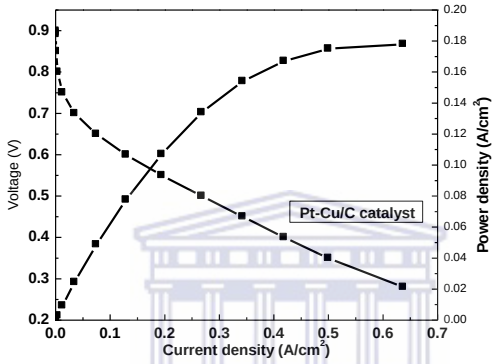

Figure 3.16 Polarization showing cell voltage and power density versus current density for an in-house MEA at 160^{o}C.

A current density of 0.13 A/cm^2, 0.268 A/cm^2 and 0.309 A/cm^2 was obtained for 140^{o}C, 160^{o}C and 180^{o}C respectively as shown in figure 3.17 The current density difference observed between 140^{o}C and 160^{o}C and between 160^{o}C and 180^{o}C is 0.138 A/cm^2 and 0.0419 A/cm^2 respectively and this shows that as the temperature increases the gaps between polarization curves for two adjacent temperatures slightly decreases. This is expected as the conductivity of the AB-PBI membrane is known to increase significantly up to 160^{o}C and then to somewhat stabilise.

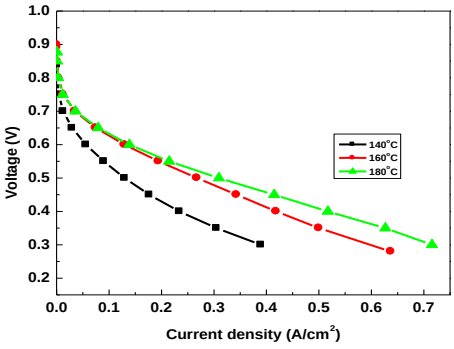

Figure 3.17 Polarization obtained with a PBI-based membrane at different temperatures using pure hydrogen as an anode gas feed.

The long term performance testing of Pt-Cu is shown in figure 3.18, showing a stable performance, in fact a slight increase throughout the operation is noted which might be due to the phosphoric acid leaving the catalyst layer and more sites access the fuel.

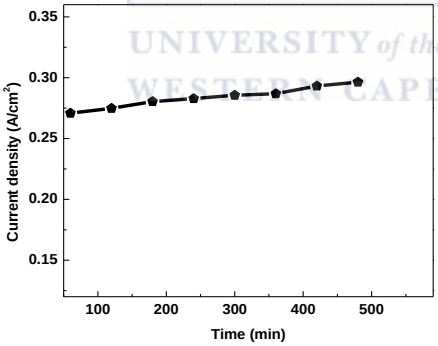

Figure 3.18 Long term performance testing of Pt-Cu/C anode catalyst.

Fuel cell curves with pure hydrogen and hydrogen containing carbon monoxide are shown in figure 3.19 for the Pt-Cu/C anode catalyst at a temperature of 160^{o}C. At the cell voltage of 0.5 V the current density decreased by 10 Ma/cm^2 from 0.27 A/cm^2 to 0.266 A/cm^{2}with 50ppm, and with 100ppm and 200 ppm a decrease of 17 Ma/cm^2 and 18 Ma/cm^2 respectively was noted. The results show that the Pt-Cu/C catalysts improve the CO tolerance of the

MEAs as compared to Pt/C, where the performance was noted to drop significantly above 50 ppm. However, CO concentration of 1000 ppm showed a considerable drop in the MEA performance, where a loss of 73 Ma/cm^2 was noted.

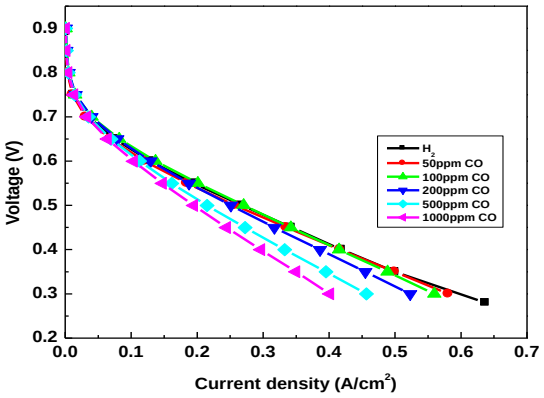

Figure 3.19 Polarization curves of a PBI-based membrane with pure hydrogen and hydrogen containing CO at 160^{o}C. The concentrations are indicated in the figure.

II. Pt-Fe/C anode catalyst

Figure 3.20 shows the performance of the in-house MEA when Pt-Fe binary catalyst, tested at different temperatures. The performance shows that at 140^{o}C a current density of 0.19 A/cm^2 was obtained at 0.5 V, with 160^{o}C and 180^{o}C giving 0.28 A/cm^2 and 0.35 A/cm^2 which is similar to that of the Pt-Cu/C catalyst.

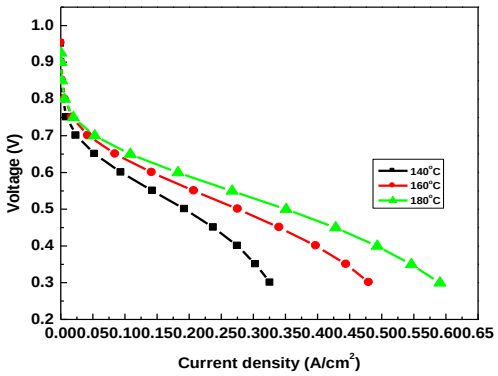

Figure 3.20 Polarization obtained with a PBI-based membrane at different temperatures using pure hydrogen as an anode gas feed.

Figure 3.21 shows the effect of CO on performance of the cell at 160°C which shows that a 50 ppm of CO in hydrogen resulted in no loss of performance, where 0.279 A/cm^{2}was recorded at 0.5V as compared to 0.28 A/cm^2 with pure hydrogen. With 100 ppm a decrease of 0.26 A/cm^2 was observed, while a maximum CO of 1000 ppm in hydrogen a loss to 0.140 A/cm^2 was noted. The results show that although at low CO concentrations the tolerance has improved for Pt-Fe/C catalysts, there is still a significant drop in performance with CO concentrations above 200 ppm.

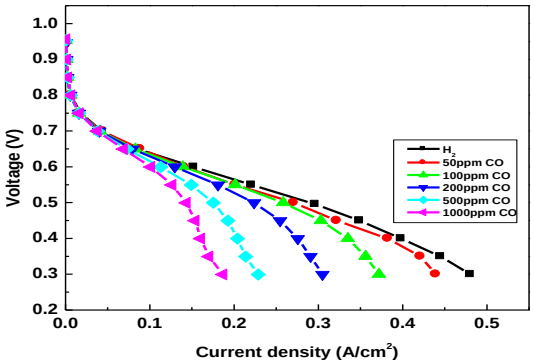

Figure 3.21 Illustration of the effect of CO on a proton exchange membrane fuel cell on Pt-Fe/C anode catalyst MEA.

III. Pt-Co/C anode catalyst

Figure 3.22 shows the performance of Pt-Co/C anode catalyst. This MEA exhibited a current density of 0.34 A/cm^2 at 0.5 V at an operating temperature of 160^{o}C. The performance is better than that of Pt-Cu/C and Pt-Fe/C. Figure 3.23 shows the performance of this MEA at different temperatures, where at 180^{o}C a current density of 0.38 A/cm^{2}was obtained 0.5 V, only an improvement of 44 Ma/cm^{2}compared to that of 160^{o}C.

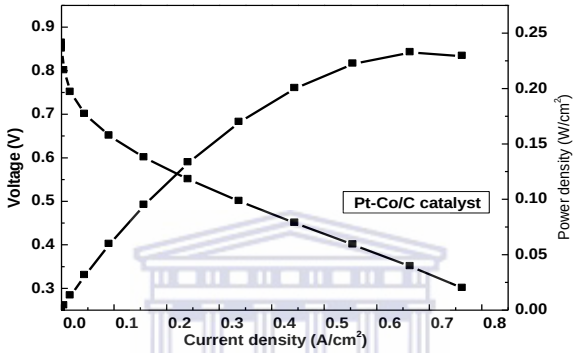

Figure 3.22 Polarization curve of Pt-Co/C anode catalyst MEA operated on H_2 at 160^{o}C

However between 140^{o}C and 160^{o}C the current density difference recorded is 150 Ma/cm^2. Thus it can be observed that the gaps between polarization curves for two adjacent temperatures decreases slightly with an increase in temperature. Also it can be seen that Pt-Co/C catalyst gave better performance compared to other Pt-alloy based anode catalyst tested in this study.

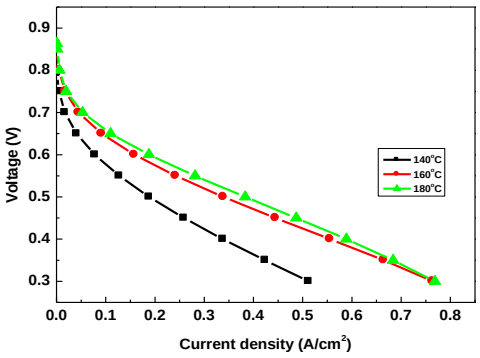

Figure 3.23 Polarization curves of Pt-Co/C anode catalyst MEA operated on H_2 at various operating temperatures.

CO concentrations were tested on Pt-Co/C anode catalyst; we can see that at the cell voltage of 0.5 V for hydrogen containing 50 ppm, the current density did not show any decrease same with 100 and 200 ppm CO. A performance loss of 6% and 9% was observed when 500 and 1000 ppm of CO was tested. When Pt-Co anode catalyst was tested for CO tolerance at 160^{o}C no significant loss in performance was observed and this indicates that the CO became dissociated from platinum reaction sites at this operation temperature which possessed a high CO tolerance and provided more catalyst sites for hydrogen. Hence no significant loss due to CO was observed with this catalyst than other bimetallic catalysts.

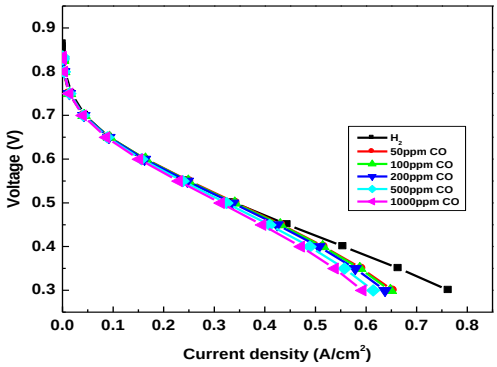

Figure 3.24 Polarization curves of a PBI-based membrane with pure hydrogen and hydrogen containing CO at 160°C. The concentrations are indicated in the figure.

IV. Pt-Ni/C anode catalyst

The performance of Pt-Ni/C binary catalyst is shown in figure 3.25, where a current density of 0.16 A/cm^2 was obtained at 0.5 V with a maximum power density of 0.14 W/cm^2. A current density of 0.089A/cm^2, 0.16 A/cm^2 and 0.21 A/cm^2 was obtained for 140°C, 160°C and 180°C respectively at 0.5 V as shown in figure 3.26. Pt-Ni/C was found to have the lowest activity compared to Pt/C and other Pt-alloy catalysts.

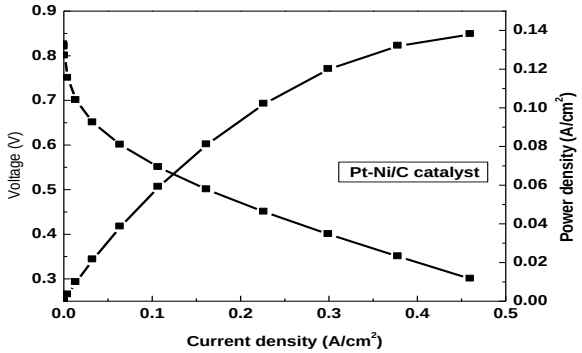

Figure 3.25 Polarization showing cell voltage and power density versus current density for a Pt-alloy based in-house MEA at 160°C.

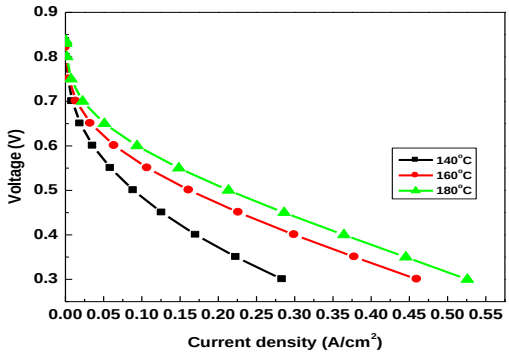

Figure 3.26 Polarization curves of Pt-Ni/C anode catalyst MEA operated on H_2 at various operating temperatures.

CO concentrations were tested on Pt-Ni/C anode catalyst; we can see from Figure 3.27 that at the cell voltage of 0.5 V for hydrogen containing 50ppm, the current density decreased from 0.16 A/cm^{2}with pure H_2 to 0.13 A/cm^2 (decreased by 19%). Similar performance was observed with 100 and 200 ppm. A drop of 25% was obtained with 1000 ppm CO.

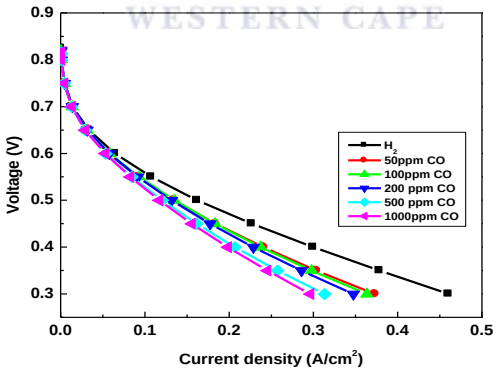

Figure 3.27 Illustration of the effect of CO on a proton exchange membrane fuel cell on Pt-Ni/C anode catalyst MEA.

The graph in figure 3.28 illustrates the comparison between Pt/C and Pt alloys based catalysts for anode. It is observed that the performance of Pt-alloy catalyst were not better than Pt/C, with Pt-Co/C showing comparable performance. This is somehow expected as the base

metals are not as active as Pt/C for hydrogen oxidation and the introduction of base metals to Pt/C would have reduced the available Pt sites for electrochemical oxidation.

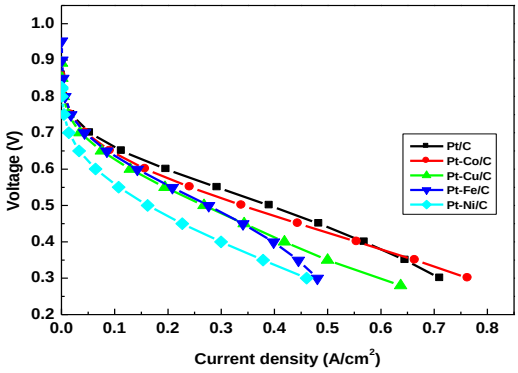

Figure 3.28 Comparison graph showing performance of Pt/C and Pt-alloy catalysts for anode obtained at 160°C.

The graph in figure 3.29 shows durability and stability of Pt/C catalyst and binary catalysts at 0.5 V and 160°C. The binary catalysts are illustrated in the figure. It is observed that Pt/C catalyst gave better performance with no significant loss. Among the binary catalyst studied, Pt-Co/C and Pt-Cu/C showed good stability, in fact an increase in the performance was noted with time. A gradual decrease in the performance is observed for Pt-Fe/C. Among the catalysts studied, Pt-Ni/C was found to have the lowest activity but the durability of all the catalysts were found to be stable under the testing conditions except for Pt-Fe/C, where a drop in the performance was noted.

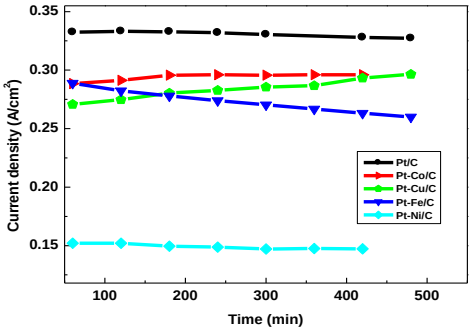

Figure 3.29 Long term performance of in-house Pt/C and binary catalysts based MEA's.

From the graph in figure 3.30 Pt-Fe/C showed higher OCV compared to other binary catalysts. The OCV degradation tests were carried out after long term durability tests. The performance of Pt/C was stable compared to the binary catalysts which showed a decline few minutes into operation. Under OCV conditions the membrane is said to suffer homogeneous degradation and resulting in massive ionomer loss and thinning of the membrane throughout the active area.

Inaba et al. [77] found that high temperature was the cause of accelerated membrane thinning under OCV and this leads to severe performance loss.

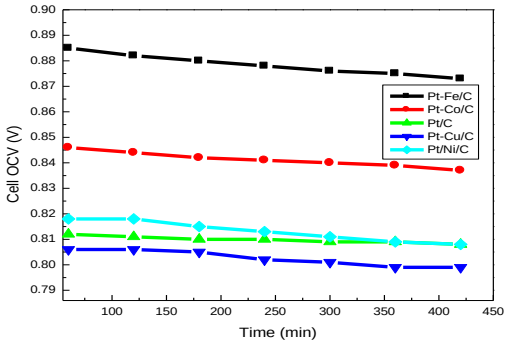

Figure 3.30 Open circuit voltage (OCV) degradation performance of in-house Pt/C and binary catalysts based MEA's.

Figure 3.31 shows GDL cross-sectional images of Pt-alloy based MEA's after the durability studies. As noted with commercial MEA, the SEM images of the in-house tested MEAs also showed that carbon is almost non-existent on the GDL. It is said that carbon supports degrade during the start-up and stopping of the cell and when there are high potentials. At high potentials the carbon oxidizes to carbon dioxide. This causes carbon corrosion which eventually leads to a decrease in performance. These corrosion mechanisms pertain to carbon used as an electrocatalyst support, but the carbon powder in the MPL can also be corroded in the environment of an operating fuel cell [71].

3.2 Morphology of GDL for binary catalysts MEAs

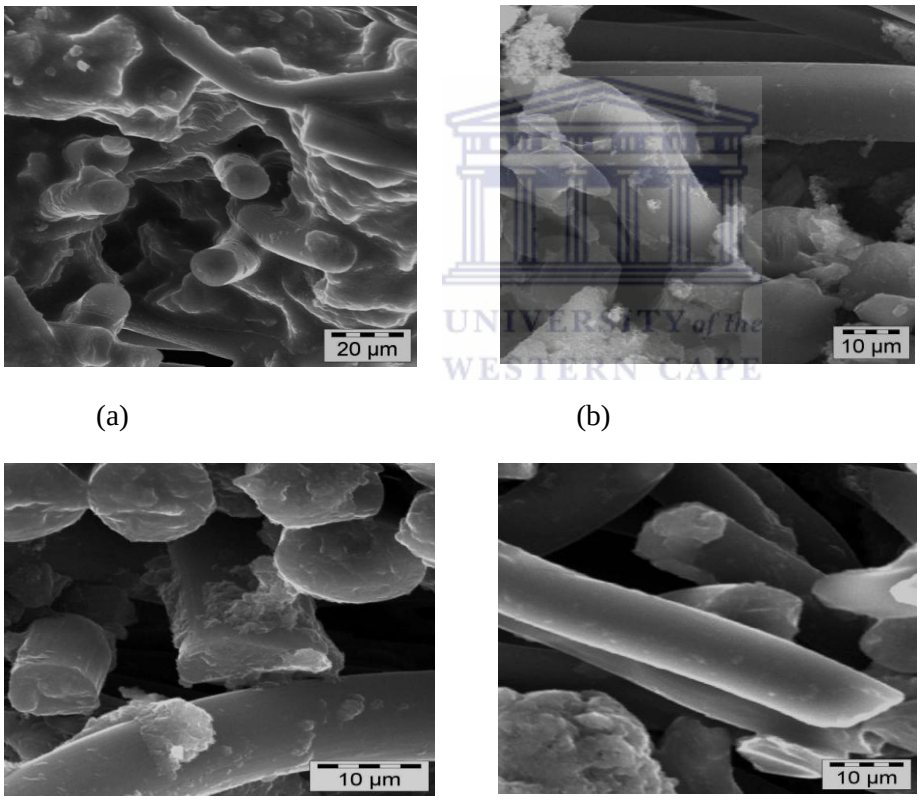

Figure 3.31 Cross sectional SEM images of GDL for (a) Pt-Co (b) Pt-Cu (c) Pt-Fe and (d) Pt-Ni binary catalysts

Figure 3.32 shows cross sectional image of the catalyst layers for the Pt-alloy anode catalysts. For all the binary catalysts some defects in the surface was noted, which might be due to the

loss of carbon from the catalyst layers that would have occurred during durability studies. From the studies it is clear that a clear drop in the performance of HTPEMFC MEAs occur when they are subjected to long-term or accelerated durability studies. Considering the operating requirements and dynamics of the fuel cell, it is imperative to improve the durability of these MEAs to realise their potential.

3.3 Morphology of catalyst layers for binary catalysts MEA's

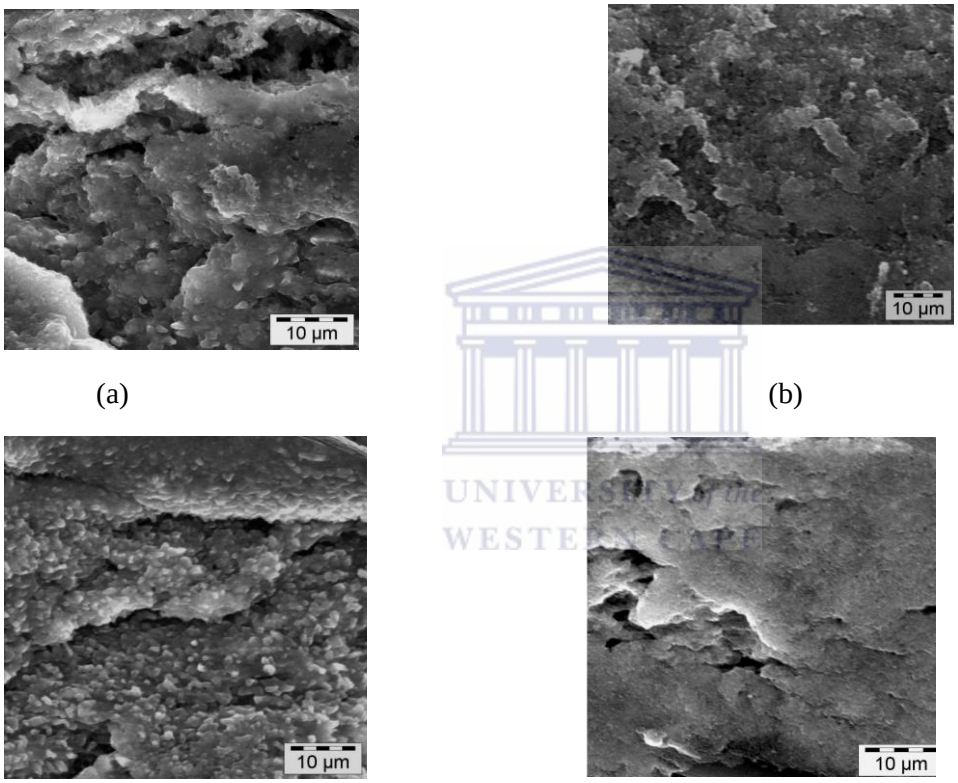

(a) (b)

© (d)

Figure 3.32 SEM image of catalyst cross-section for (a)Pt-Co/C, (b) Pt-Cu/C, (c) Pt-Ni/C and (d) Pt-Fe/C anode catalysts.

Chapter 4: Conclusion and recommendations

4.1 Conclusions

The study is focussed on the durability analysis of a commercial MEA. The performance/durability of the commercial MEA is then compared to that of an in-house developed MEA. Several binary catalysts were used for the in-house MEA, particularly on the anode side, hoping to improve the CO tolerance of the MEA's.

The commercial MEA performance was good considering the polarization experiments were carried out under dry H_2/Air supply and at atmospheric pressures. The MEA also showed good long-term stability. However, the CO tolerance was limited to only 50 ppm as further increase in the CO concentration found to affect the performance significantly. The most important finding is that the major factor contributing to the loss in the performance of HTPEM MEAs is the temperature cycling/dynamics in the operating condition of the fuel cell. An 80% drop in the performance was noted just after four cycles between 40-160^{o}C. The reason for the drop could have been the loss of phosphoric acid from the catalyst layer and the membrane due to these cycles. SEM results also showed that almost all carbon on the GDL layer have oxidised and disappeared during the analysis. Also cracks/potholes were noted in the catalyst layer after the long-term studies indicating a loss of carbon. Loss of carbon from the catalyst layer will result in the Pt particles agglomerating leading to a loss in surface area. Therefore, either the corrosion of carbon should be prevented or an alternative support has to be identified to solve the durability issues of AB-PBI based HTPEMFC MEA's. Also SEM studies indicated a thinning of the membrane, which may be due to the attack by HO• and HO_2• radicals produced by the incomplete reduction of oxygen on the cathode side. Therefore, it has to be understood that the durability of the HTPEMFC MEA is

affected by various parameters and all of them should be taken into account while designing a suitable HTPEMFC MEA.

In-house MEAs were prepared and evaluated, including Pt-alloy catalysts as anodes to improve the CO tolerance. The in-house Pt/C based MEA, albeit slightly lower, showed comparable performance to commercial MEA. The CO tolerances of both in-house and commercial MEAs were comparable. The performance and CO tolerance of the binary catalyst based MEAs were specific to the catalysts used, with Pt-Co/C showing reasonable performance and excellent CO tolerance as compared to the other catalysts.

4.2 Recommendations

- Further work should be performed to understand the sudden drop in the performance of HTPEMFC MEAs during temperature cycling.
- Degradations of PEMFC components under various operation conditions must be understood, this may require durability investigation of one component at a time, for example carbon oxidation or membrane thinning, or platinum agglomeration, mechanical stress etc.
- Novel characterization techniques need to be developed and employed to understand which parameter affects the durability the most apart from temperature cycling, is it carbon corrosion, membrane thinning or catalyst agglomeration and thereby develop suitable methods to prevent them.

Chapter 5: References

1. Johansson, T.B., Kelly, H., Reddy, A.K.N ,and Williams, R.H. *Renewable Energy: Sources for Fuels and Electricity*,**204** (1993) 9-13

2. The Future of the Hydrogen Economy, Bright or Bleak?" by Ulf Bossel, Baldur Eliasson and Gordon Taylor, April 2003, *www.efcf.com/reports*.

3. L. Carrette, K. A. Friedrich and U. Stimming, *Fuel cells - fundamentals and applications, Fuel Cells*, **1(1)**, 2001, 5-39

4. L. Carrette, K. A. Friedrich and U. Stimming, *Fuel cells - fundamentals and applications, Fuel Cells*, **3(4)**, 2001, 5-39

5. Barbir, F., *PEM Fuel Cells: Theory and Practice*, Elsevier Academic Press, (2005), 356-372

6. *http://www.che.sc.edu/centers/PEMFC/about_fuelcell_1.html*

7. Barbir, F. & Gómez, T., 1997. *Efficiency and Economics of PEM Fuel Cells.International Journal of Hydrogen Energy*. **Vol.22**, no. 10/11. pp. 1027-1038.

8. L. Carrette, K. A. Friedrich and U. Stimming, Fuel cells - fundamentals and applications, Fuel Cells, **1(1)**, 2001, 67-78.

9. Yuan.X.Z., W. *PEM Fuel Cell Fundamentals*. London: Springer London. (2008).183, 260

10. Kuang, K., &Easler, K., *Fuel Cell Electronics Packaging*. San diego: Springer, (2007), 996-1002

11. Xiao, L., Zhang, H., Scanlon, E., Ramanathan, L., Choe, E., Rogers, D., *High temperature polybenzimidazole fuel cell membranes via a sol-gel process*, Chem. Master. **17**, (2005), pp. 5328-33.

12. Li, X., *Principles of Fuel Cells*, New York: Taylor & Francis Group, (2006), 29-36

13. Cheng Xiaoliang, Yi Baolian, Han Ming, Zhang Jingxin, Qiao Yaguang, Yu Jingrong, 1999. *Investigation of platinum utilization and morphology in catalyst layer of polymer electrolyte fuel cells*. Journal of Power Sources, Vol. **79**, No. 1, pp. 75-81

14. Zhang, J., *PEM Fuel Cell Electrocatalysts and Catalyst Layers, Fundamentals and Applications*, Canada: Springer, (2008), 685.

15. Melis, A and Happe, T., *Hydrogen Production: Green Algae as a Source of Energy. Plant Physiology*, (2001) Volume **127**: pp.740-748

16. *http:www.energi.kemi.dtu.dk/Projekter/fuelcells.aspx*

17. Zawodzinski, T.A.,Jr.; Springer, T.E.; Davey, J.; Jestel, R.; Lopez, C.; Valerio, J.; Gottesfeld, S. *A comparative study of water uptake by and transport through ionomeric fuel cell membranes. J. Electrochem. Soc*. (1993), 140.

18. Panchenko, A., *Polymer Electrolyte Membrane Degradation and Oxidant Reduction in Fuel Cells: an EPR and DFT investigation, PhD Thesis*, Institute fürPhzsikalischeChemie der Universitat, (2004), p26.

19. Y.G. Chun, C.S. Kim, D.H. Peck, D.R. Shin, *Journal Power Sources*, (1998) 71, 174

20. Zhang, J., *PEM Fuel Cell Electrocatalysts and Catalyst Layers, Fundamentals and Applications*, Canada: Springer, (2008), 361.

21. Schulze, M.; Wagner, N.; Kaz, T.; Friedrich, K. A., *Combined electrochemical and surface analysis investigation of degradation processes in polymer electrolyte membrane fuel cells*, (2002), p119.

22. Weber, A. Z.; Newman, J., *Effects of microporous layers in polymer electrolyte fuel cells. Journal of the Electrochemical Society* 2005, **152 (4)**, A677-A688

23. Zhang, H.; Wang, X.; Zhang, J.; Zhang, J., *Conventional Catalyst Ink, Catalyst Layer, and MEA Preparation. In PEM fuel cell electrocatalysts and catalyst layers: fundamentals and applications*; Zhang, J., Ed. Springer: London (2008) pp 889-916

24. D. P. Wiklinson and J. St-Pierre, *Durability, Handbook of fuel cells - fundamentals, technology, applications*, (2003), 196-220.

25. Davies, D., Adcock, P., Turbin, M., &Rowen, S., *Stainless Steel as a Bipolar Plate Material for Solid Polymer Fuel Cells, Journal of Power Sources***86** (2000), pp. 237-42

26. A. Hermann, T. Chaudhuri, P. Spagnol, *Int. J. Hydrogen Energy***30** (2005)1297–1302

27. T.V. Nguyen and R.E. White *Journal of Electrochemical Society*, 140(8), pp.2178-2186, 1993.

28. K. Adjemian, S. Lee, S. Srinivasan, J. Benziger, and A. Bocarsly, *J. Electrochem. Soc*., **149**, A256 (2002).

29. Jiri Koziorek, BohumilHorak and MiroslavKopriva , VSB-TU of Ostrava, *Faculty of Engineering and Computer Science Czech Republic, Control of fuel cell systems in mobile applications*,**38** (2003) p.195-200

30. K.C.Neyerlin, H.A.Gasteiger, C.K.Mittelsteadt, J.Jorne, W.Gu. *Effect of relative humidity on oxygen reduction kinetics in a PEMFC. Journal of The Electrochemical Society***152**(2005) 1073-1080

31. S. Thomas, M. Zalbowitz, *Fuel cells - Green Power. 2000*, Los Alamos National Laboratory: New Maxico

32. Yousfi-Steiner.N., O. C. *A review on PEM voltage degradation associated with water management: impacts, influence factors and characterization. Journal of Power Source*, (2008) 183, 260.

33. Barbir, F., *PEM Fuel Cells: Theory and Practice*, Elsevier Academic Press, (2005), 364.

34. R.J. Wayne, *Durability Studies on Polymer Electrolyte Membrane Fuel Cells, in Department of Materials Science and Engineering*. 2004, Case Western Reserve University. p.120

35. Kerres JA. *Development of ionomer membranes for fuel cells*, J MemberSci **185** (2001), 3 –27.

36. *http://www.grin.com/en/doc/277526/membrane-degradation-studies-in-pemfcs*

37. M.W.Fowler, R.F.Mann, J.C.Amphlett, B.A.Peppley, P.R.Roberge. *Incorporation of voltage degradation into a generalised steady state electrochemical model for a PEM fuel cell. Journal of Power Sources* **106** (2002), 274-283.

38. Hamrock SJ, Yandrasits MA. *Proton exchange membranes for fuel cell applications*, Polymer Rev **46(3)** (2006) 219–44

39. P.E Cassidy, *Thermally stable Polymers*, 1980,Marcel Dekker Inc., NY 5,109

40. J.A. Asensio, S. Borros, P. Gomez-Romeo, *Journal of Electrochemistry Soc*. 2003, pp 151 A304

41. X. Cheng, Z. Shi, N. Glass, L. Zhang, J. Zhang, D. Song, Z.-S. Liu, H. Wang, J. Shen, *J. Power Sources* **99** (2007), 165,739

42. Stucki, S.; Scherer, G. G.; Schlagowski, S.; Fischer, E. J. Appl. Electrochem. (1998), 28, 1041

43. Borup, R.L., et.al., *PEM fuel cell electrocatalyst durability measurements, Journal of Power Sources,***166(1)(**2007). p.149-164

44. Fuller TF, Gray G. *Carbon corrosion induced by partial hydrogen coverage*. ECS Trans **1(8)** (2006) 345–53

45. Antolini, E., *Formation microstructural characteristics and stability of carbon supported platinum catalysts for low temperature fuel cells. Journal of Materials Science*, **38(14)** 2003 pg. 2995-3001

46. H.A. Gasteiger, A. Lamm (Eds.), *Handbook of Fuel Cells: Fundamentals Technology and Applications*, vol. **3**, John Wiley & Sons Ltd., 2003, pp. 663

47. Samms SR, Wasmus S, Savinell RF. *Thermal stability of Nafion in simulated fuel cell environments. J ElectrochemSoc* **143(5)** (1996) 1498–504.

48. Sompalli B, Litteer BA, Gu WB, Gasteiger HA. *Membrane degradation at catalyst layer edges in PEMFC MEAs. J ElectrochemSoc* **154(12)** (2007) 1349–57.

49. Tang YH, Zhang JL, Song CJ, Zhang JJ. *Single PEMFC design and validation for high-temperature MEA testing and diagnosis*. *Electrochem Solid-State* Lett (2007), 142–169

50. J. A. Asensio, S.Borros, P.Gomez-Romeo, *J.Electrochem.Soc*2003, 150 A304.

51. Huang XY, Solasi R, Zou Y, Feshler M, Reifsnider K, Condit D, et al. *Mechanical endurance of polymer lectrolyte membrane and PEM fuel cell durability. J PolymSci* Part B: PolymPhys 2006; 2346

52. Schiraldi DA. *Perfluorinated polymer electrolyte membrane durability*. Polymer Rev (2006) 315–279

53. Kangasniemi KH, Condit DA, Jarvi TD. *Characterization of vulcan electrochemically oxidized under simulated PEM fuel cell conditions*. J ElectrochemSoc 2004 **151**(4):E125–32

54. Maass S, Finsterwalder F, Frank G, Hartmann R, Merten C. *Carbon support oxidation in PEM fuel cell cathodes. Journal Power Sources* 2008 444–51

55. Rong F, Huang C, Liu Z-S, Song DT, Wang QP. *Microstructure changes in the catalyst layers of PEM fuel cells induced by load cycling part I mechanical model. J Power Sources*(2008), 699–711

56. Garzon FH, Rockward T, Urdampilleta IG, Brosha EL, Uribe FA. *The impact of hydrogen fuel contaminates on long-term PEMFC performance*. ECS Trans 2006;3(1): 695–703.

57. Cheng X, Shi Z, Glass N, Zhang L, Zhang JJ, Song DT, et al. *A review of PEM hydrogen fuel cell contamination: impacts, mechanisms, and mitigation. J Power Sources* 2007, 739–556

58. M. Murthy, M. Esayian, A. Hobson, S. MacKenzie, W. Lee, and J. W. Van Zee, *Journal of Electrochem. Soc*., **148**, (2001) A1141

59. B. N. Grgur, N. M. Markovi}, C. A. Lucas, P. N. Ross Jr, J. Serb. *Chem. Soc*. **66** (2001) 785

60. H. Igarashi, T. Fujino, and M. Watanabe, J. Electroanal. Chem., 391 (1995) 119

61. Tang Y, Zhang J, Song C, Liu H, Wang H, et al. *PEM Fuel cell electrocatalysts and catalysts, Fundamentals and applications*, NRC 4250 Wesbrook Mall Canada, 2008, pg 988.

62. Van Helleputte. H.R.J.R, Haddeman.T.B.J, Verheijen.M.J, Baalbergen. J.-J.*Microelectronic Engineering*, **27** (1995) 547-550.

63. Godfrey, Douglas, *"Review of Usefulness of New Surface Analysis Instruments in Understanding Boundary Lubrication"*, Proc. of the International Conf. on the Fundamentals of Tribology, Eds. N.P. Suh and N. Saka, MIT Press , Cambridge Mass. (1980), pp. 945 -967.

64. E. Endoh, S. Terazono, H. Widjaja, and Y. Takimoto, *Electrochem. Solid-State Lett*., **7**, A209 2004.

65. Curtin DE, Lousenberg RD, Henry TJ, Tangeman PC, Tisack ME. *Advanced materials for improved PEMFC performance and life. Journal Power Sources* 2004; **131** (1–2):41–8.

66. Yuyan Shao, G.Y., Zhenbo Wang, YunzhiGao, *Proton exchange membrane fuel cell from low temperature to high temperature: Material challenges. Journal of Power Sources* **167** (2007) p. 235-242.

67. Jens Oluf Jensen, DTU Qingfeng Li, DTU Carina Terkelsen, DPS Hans Christian Rudbech, *DPS Development of HT-PEMFC Components and Stack For CHP Unit, Project* 7328 PSO R&D 2007 programme, p1011-1015

68. S. Gottesfeld, and J. Pafford, J. Electrochem. Soc., **135** (1988) p 2651

69. S.Kundu, M.W Fowler, L.C Simon, S Grot, *Journal of Power Sources*, Vol. **157**, issue 2, p. 650-656

70. E. Endoh, S. Terazono, H. Widjaja, Y. Takimoto, *Electrochem. Solid-State Lett*. **7** (2004) A209–A211

71. Q. Guo, P.N. Pintauro, H. Tang, S. O'onnor, *J. Power Sources* **154** (1999) 175

72. Beuscher U, Cleghorn SJC, Johnson WB. *Challenges for PEM fuel cell membranes. Int J Energy Res* **29 (12)** (2005) 1103–12.

73. Liu W, Zuckerbrod D. *In situ detection of hydrogen peroxide in PEM fuel cells. J Electrochem Soc* **152 (6)** (2005) A1165–70.

74. Rong F, Huang C, Liu Z-S, Song DT, Wang QP. *Microstructure changes in the catalyst layers of PEM fuel cells induced by load cycling part I mechanical model. J Power Sources* **175 (2)** (2008) 699–711.

75. Borup R, Meyers J, Pivovar B, Seung Kim Y, Mukundan R, Garland N, et al. *Scientific aspects of polymer electrolyte fuel cell durability and degradation. Chem Rev* **107 (10)** (2007) 3904–51.

76. Dam VAT, de Bruijn FA. *The stability of PEMFC electrodes platinum dissolution vs potential and temperature investigated by quartz crystal microbalance. J Electrochem Soc* **154 (5)** (2007) B494–9.

77. Inaba M, Kinumoto T, Kiriake M, Umebayashi R, Tasaka A, Ogumi Z. *Gas crossover and membrane degradation in polymer electrolyte fuel cells. Electrochim Acta* **51(26)** (2006) 5746–53